New Physics signatures in Rare Decays from LHCb

Marcin Chrząszcz
mchrzasz@cern.ch

University of Zurich[UZH]

University of Adelaide
October 25, 2016

Outline

1. Why flavour is important.
2. LHCb detector.
3. $b \to s\ell\ell$ theory in a nutshell.
4. LHCb measurements of $B^0_d \to K^*\mu\mu$
   - Maximum likelihood fit.
   - Method of moments.
   - Amplitudes fit.
5. Other related LHCb measurements.
6. Global fit to $b \to s\ell\ell$ measurements.
7. Disclaimers about some theory predictions.
8. Conclusions.

Why Flavour is important?

A lesson from history - GIM mechanism

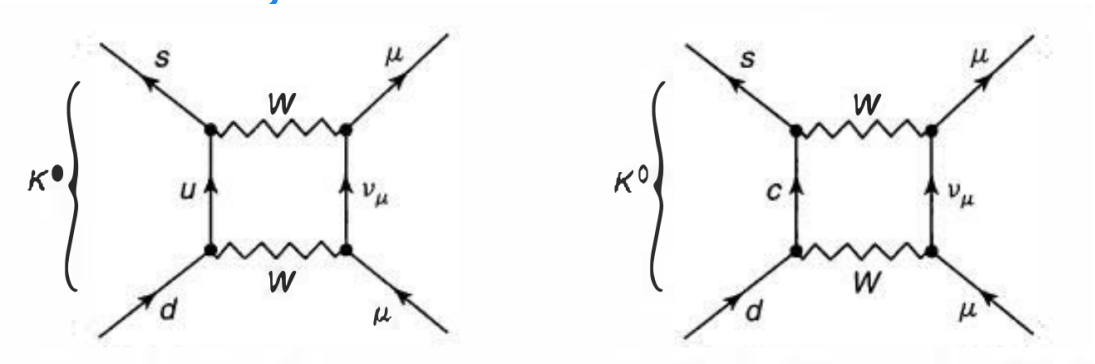

- Cabibbo angle was successful in explaining dozens of decay rates in the 1960s.
- There was, however, one that was not observed by experiments: $K^0 \to \mu^- \mu^+$.
- Glashow, Iliopoulos, Maiani (GIM) mechanism was proposed in the 1970 to fix this problem. The mechanism required the existence of a 4^{th} quark.
- At that point most of the people were skeptical about that. Fortunately in 1974 the discovery of the J/ψ meson silenced the skeptics.

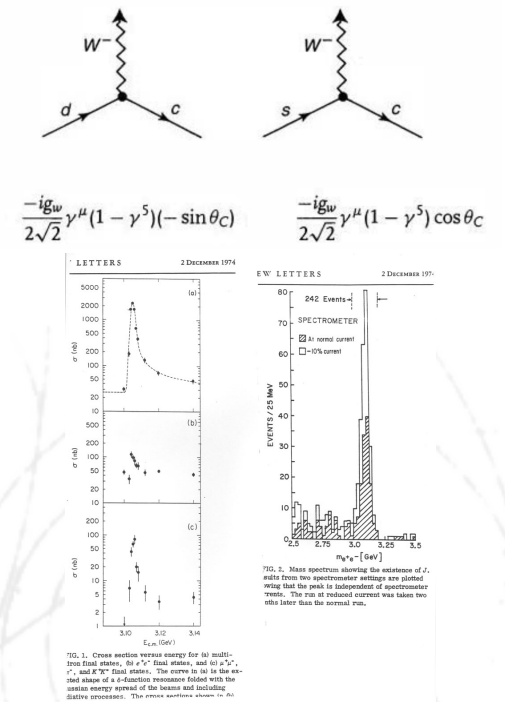

A lesson from history - CKM matrix

$$V \approx \begin{pmatrix} 1 & \lambda & \lambda^3 \\ -\lambda & 1 & \lambda^2 \\ -\lambda^3 & -\lambda^2 & 1 \end{pmatrix} \begin{matrix} u \\ c \\ t \end{matrix}$$

$\lambda \approx 0.22$: Cabibbo angle

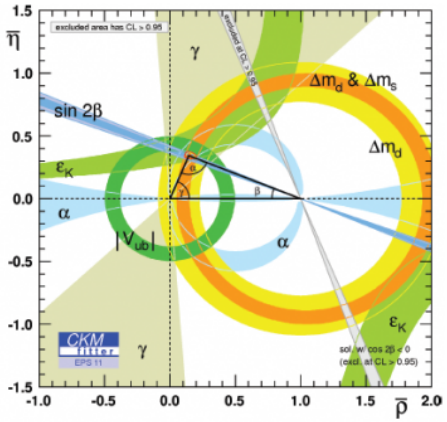

- Similarly, CP violation was discovered in 1960s in the neutral kaons decays.
- 2×2 Cabbibo matrix could not allow for any CP violation.
- For CP violation to be possible one needs at least a 3×3 unitary matrix
  ↬ Cabibbo-Kobayashi-Maskawa matrix (1973).
- It predicts existence of b (1977) and t (1995) quarks.

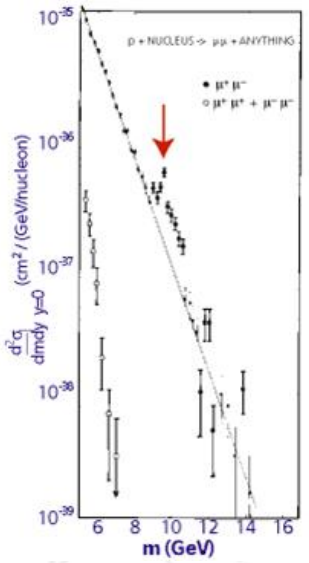

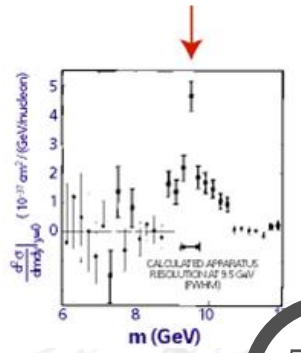

A lesson from history - Weak neutral current

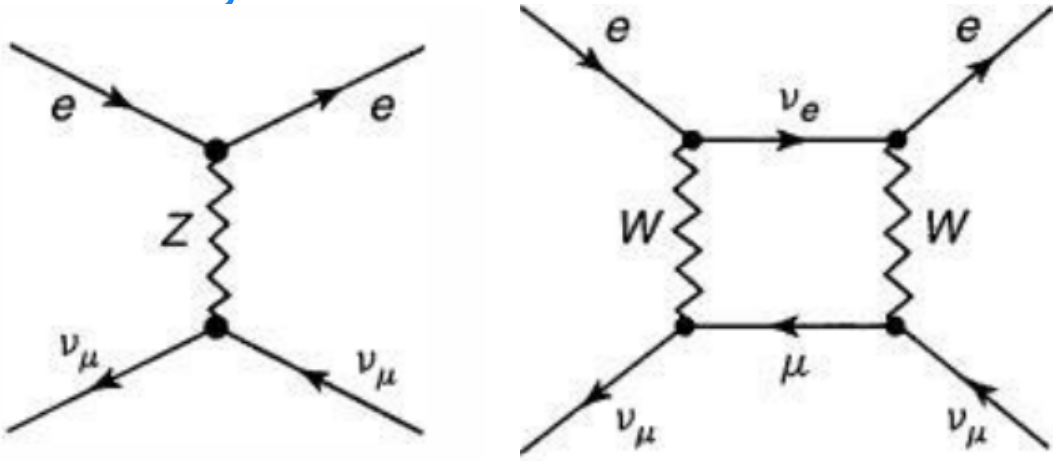

- Weak neutral currents were first introduced in 1958 by Buldman.
- Later on they were naturally incorporated into unification of weak and electromagnetic interactions.
- 't Hooft proved that the GWS models was renormalizable.
- Everything was there on theory side, only missing piece was the experiment, till 1973.

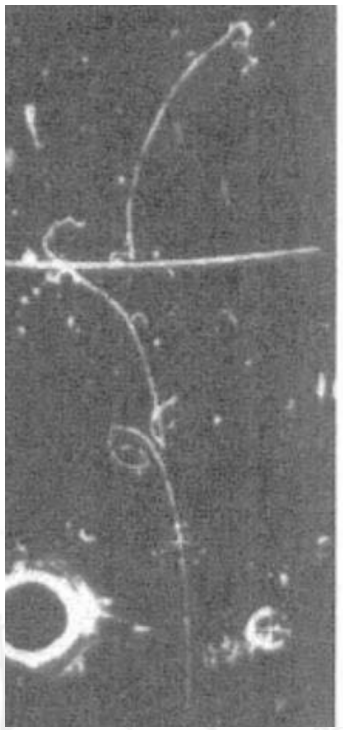

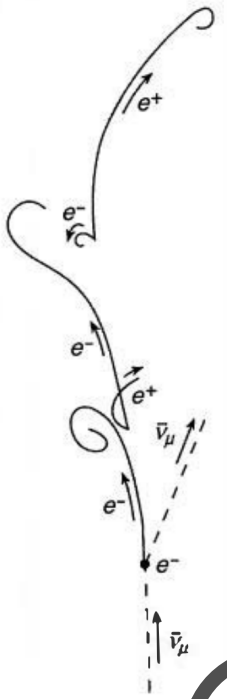

LHCb detector

LHCb detector - tracking

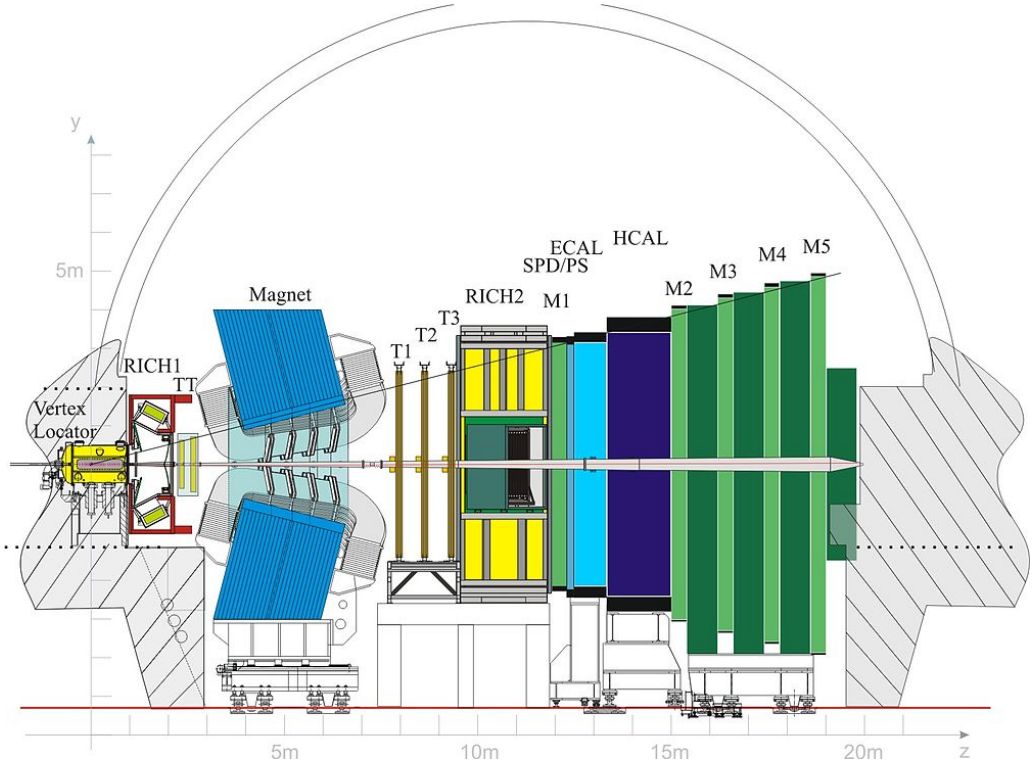

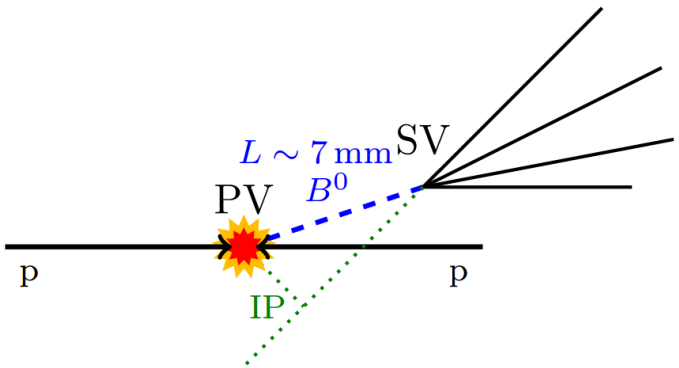

- Excellent Impact Parameter (IP) resolution ($20\ \mu\mathrm{m}$).
  $\Rightarrow$ Identify secondary vertices from heavy flavour decays
- Proper time resolution $\sim\ 40\ \mathrm{fs}$.
  $\Rightarrow$ Good separation of primary and secondary vertices.
- Excellent momentum ($\delta p/p \sim 0.4 - 0.6\%$) and inv. mass resolution.
  $\Rightarrow$ Low combinatorial background.

LHCb detector - particle identification

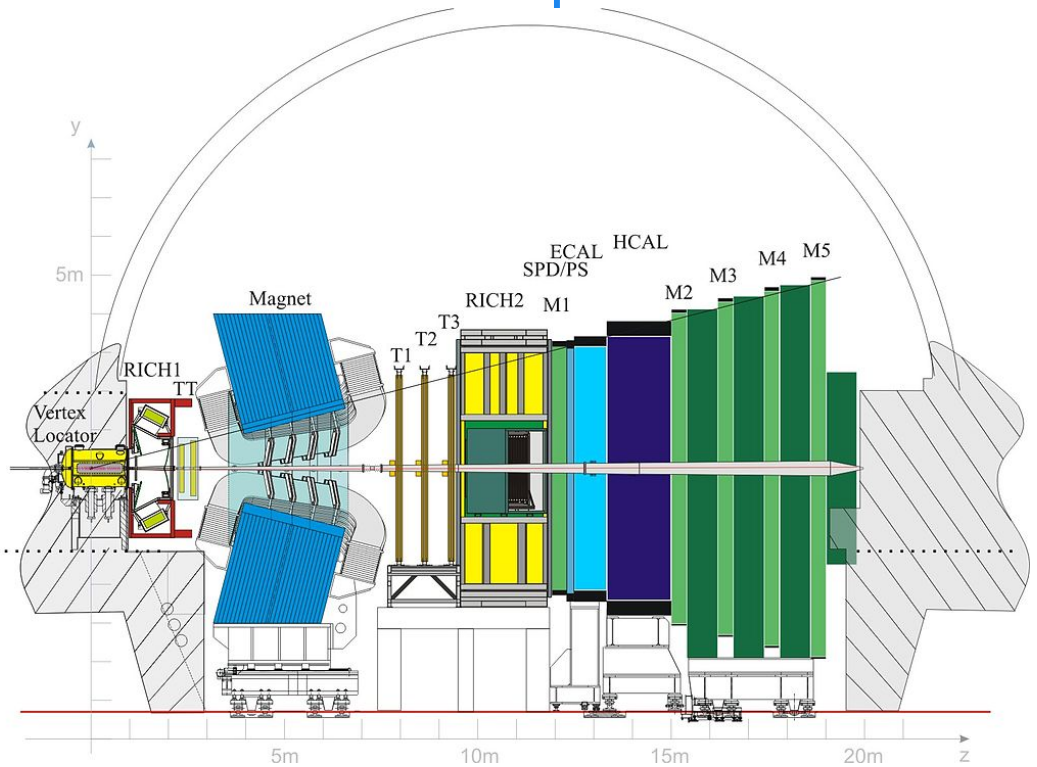

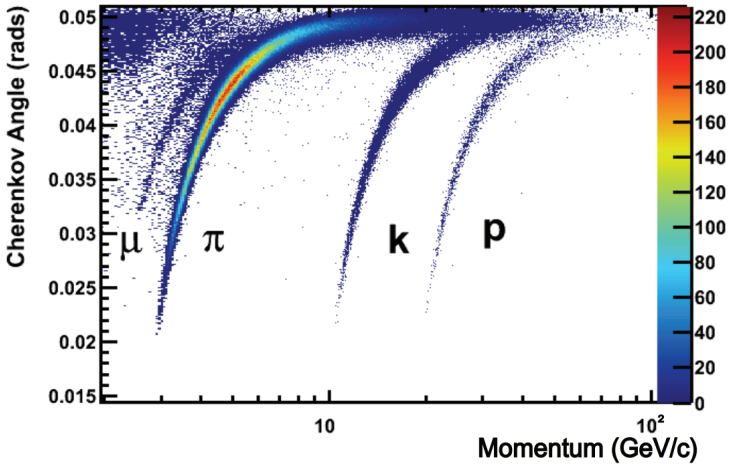

- Excellent Muon identification $\epsilon_{\mu\to\mu} \sim 97\%$, $\epsilon_{\pi\to\mu} \sim 1-3\%$
- Good $K-\pi$ separation via RICH detectors, $\epsilon_{K\to K} \sim 95\%$, $\epsilon_{\pi\to K} \sim 5\%$.
  $\Rightarrow$ Reject peaking backgrounds.
- High trigger efficiencies, low momentum thresholds. Muons:
  $p_T > 1.76\mathrm{GeV}$ at L0, $p_T > 1.0\mathrm{GeV}$ at HLT1,
  $B \to J/\psi X$: Trigger $\sim 90\%$.

$b \to s\ell\ell$ theory in a nutshell.

Why rare decays?

- The SM allows only the charged interactions to change flavour.
  - Other interactions are flavour conserving.
- One can escape this constraint and produce $b \to s$ and $b \to d$ at loop level.
  - These kind of processes are suppressed in SM → Rare decays.
  - New Physics can enter in the loops.

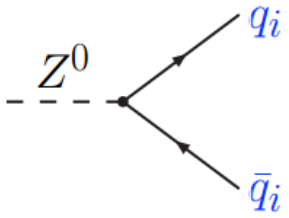

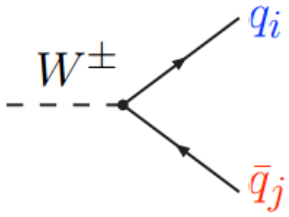

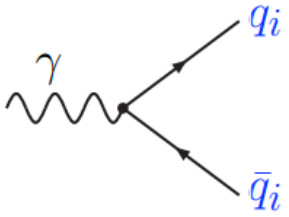

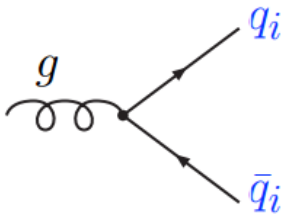

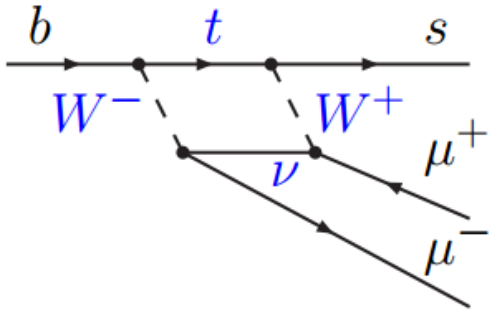

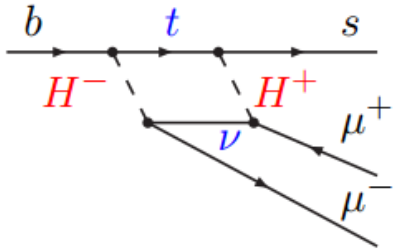

Tools in rare B^0 decays

- **Operator Product Expansion and Effective Field Theory**

$$H_{eff} = -\frac{4G_f}{\sqrt{2}} V V'^* \sum_i \left[\underbrace{C_i(\mu) O_i(\mu)}_{\text{left-handed}} + \underbrace{C'_i(\mu) O'_i(\mu)}_{\text{right-handed}} \right],$$

i=1,2	Tree
i=3-6,8	Gluon penguin
i=7	Photon penguin
i=9.10	EW penguin
i=S	Scalar penguin
i=P	Pseudoscalar penguin

where C_i are the Wilson coefficients and O_i are the corresponding effective operators.

$b \to s\gamma$

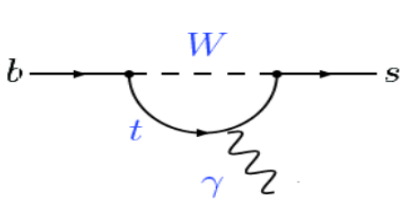

$C_7^{(\prime)}$

$b \to s\ell^+\ell^-$

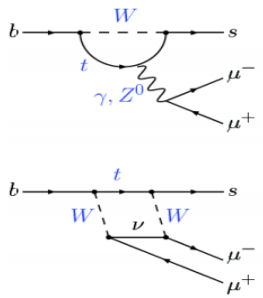

$C_7^{(\prime)}, C_9^{(\prime)}, C_{10}^{(\prime)}$

$B^0_{(s)} \to \mu^+\mu^-$

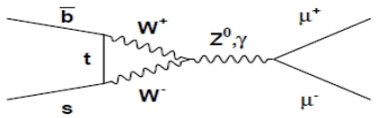

$C_S^{(\prime)}, C_P^{(\prime)}, C_{10}^{(\prime)}$

Analysis of Rare decays

Analysis of FCNC in a model-independent approach, effective Hamiltonian:

$$b \to s\gamma(^*) : \mathcal{H}^{SM}_{\Delta F=1} \propto \sum_{i=1}^{10} V^*_{ts} V_{tb} \mathcal{C}_i \mathcal{O}_i + \dots$$

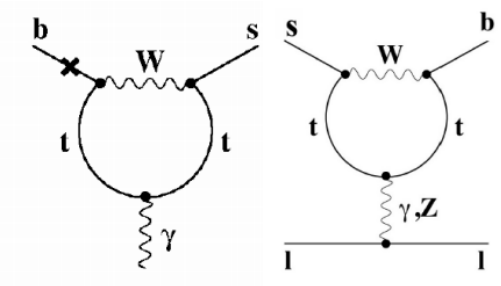

- $\mathcal{O}_7 = \frac{e}{16\pi^2} m_b \, (\bar{s}\sigma^{\mu\nu} P_R b) F_{\mu\nu}$
- $\mathcal{O}_9 = \frac{e^2}{16\pi^2} (\bar{s}\gamma_\mu P_L b) \, (\bar{\ell}\gamma_\mu \ell)$
- $\mathcal{O}_{10} = \frac{e^2}{16\pi^2} (\bar{s}\gamma_\mu P_L b) \, (\bar{\ell}\gamma_\mu \gamma_5 \ell)$, ...

• **SM** Wilson coefficients up to NNLO + e.m. corrections at $\mu_{ref} = 4.8$ GeV [Misiak et al.]:

$$\mathcal{C}_7^{\rm SM} = -0.29, \, \mathcal{C}_9^{\rm SM} = 4.1, \, \mathcal{C}_{10}^{\rm SM} = -4.3$$

• **NP** changes short distance $\mathcal{C}_i - \mathcal{C}_i^{\rm SM} = \mathcal{C}_i^{\rm NP}$ and induce new operators, like

$\mathcal{O}'_{7,9,10} = \mathcal{O}_{7,9,10} \; (P_L \leftrightarrow P_R)$ ... also scalars, pseudoescalar, tensor operators...

$B^0 \to K^*\mu^-\mu^+$ kinematics

⇛ The kinematics of $B^0 \to K^*\mu^-\mu^+$ decay is described by three angles θ_l, θ_k, ϕ and invariant mass of the dimuon system (q^2).

⇛ $\cos\theta_k$: the angle between the direction of the kaon in the K^* ($\overline{K^*}$) rest frame and the direction of the K^* ($\overline{K^*}$) in the B^0 ($\overline{B}^0$) rest frame.

⇛ $\cos\theta_l$: the angle between the direction of the μ^- (μ^+) in the dimuon rest frame and the direction of the dimuon in the B^0 ($\overline{B}^0$) rest frame.

⇛ ϕ: the angle between the plane containing the μ^- and μ^+ and the plane containing the kaon and pion from the K^*.

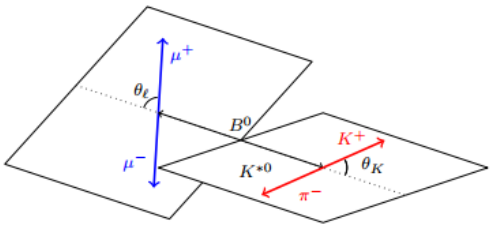

(a) θ_K and θ_ℓ definitions for the B^0 decay

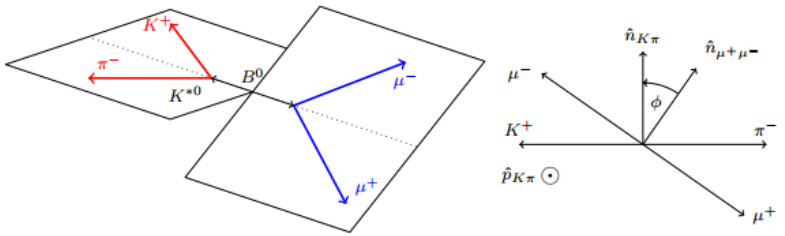

(b) ϕ definition for the B^0 decay

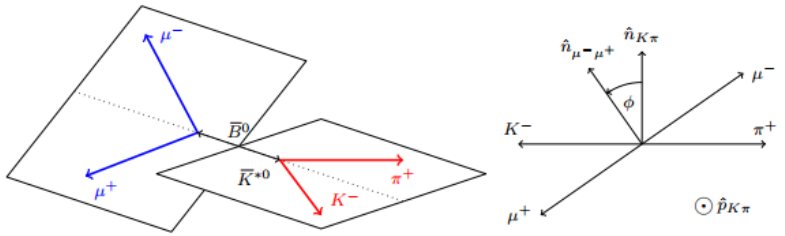

(c) ϕ definition for the $\overline{B}^0$ decay

$B^0 \to K^*\mu^-\mu^+$ kinematics

⇛ The kinematics of $B^0 \to K^*\mu^-\mu^+$ decay is described by three angles θ_l, θ_k, ϕ and invariant mass of the dimuon system (q^2).

$$\frac{d^4\Gamma}{dq^2\, d\cos\theta_K\, d\cos\theta_l\, d\phi} = \frac{9}{32\pi}\Big[J_{1s}\sin^2\theta_K + J_{1c}\cos^2\theta_K + (J_{2s}\sin^2\theta_K + J_{2c}\cos^2\theta_K)\cos 2\theta_l$$
$$+J_3\sin^2\theta_K\sin^2\theta_l\cos 2\phi + J_4\sin 2\theta_K\sin 2\theta_l\cos\phi + J_5\sin 2\theta_K\sin\theta_l\cos\phi$$
$$+(J_{6s}\sin^2\theta_K + J_{6c}\cos^2\theta_K)\cos\theta_l + J_7\sin 2\theta_K\sin\theta_l\sin\phi + J_8\sin 2\theta_K\sin 2\theta_l\sin\phi$$
$$+J_9\sin^2\theta_K\sin^2\theta_l\sin 2\phi\Big],$$

⇛ This is the most general expression of this kind of decay.

Transversity amplitudes

$\Rightarrow$ One can link the angular observables to transversity amplitudes

$$J_{1s} = \frac{(2+\beta_\ell^2)}{4}\left[|A_\perp^L|^2 + |A_\parallel^L|^2 + |A_\perp^R|^2 + |A_\parallel^R|^2\right] + \frac{4m_\ell^2}{q^2}\mathrm{Re}\left(A_\perp^L A_\perp^{R*} + A_\parallel^L A_\parallel^{R*}\right),$$

$$J_{1c} = |A_0^L|^2 + |A_0^R|^2 + \frac{4m_\ell^2}{q^2}\left[|A_t|^2 + 2\mathrm{Re}(A_0^L A_0^{R*})\right] + \beta_\ell^2 |A_S|^2,$$

$$J_{2s} = \frac{\beta_\ell^2}{4}\left[|A_\perp^L|^2 + |A_\parallel^L|^2 + |A_\perp^R|^2 + |A_\parallel^R|^2\right], \qquad J_{2c} = -\beta_\ell^2\left[|A_0^L|^2 + |A_0^R|^2\right],$$

$$J_3 = \frac{1}{2}\beta_\ell^2\left[|A_\perp^L|^2 - |A_\parallel^L|^2 + |A_\perp^R|^2 - |A_\parallel^R|^2\right], \qquad J_4 = \frac{1}{\sqrt{2}}\beta_\ell^2\left[\mathrm{Re}(A_0^L A_\parallel^{L*} + A_0^R A_\parallel^{R*})\right],$$

$$J_5 = \sqrt{2}\beta_\ell\left[\mathrm{Re}(A_0^L A_\perp^{L*} - A_0^R A_\perp^{R*}) - \frac{m_\ell}{\sqrt{q^2}}\mathrm{Re}(A_\parallel^L A_S^* + A_\parallel^{R*} A_S)\right],$$

$$J_{6s} = 2\beta_\ell\left[\mathrm{Re}(A_\parallel^L A_\perp^{L*} - A_\parallel^R A_\perp^{R*})\right], \qquad J_{6c} = 4\beta_\ell\frac{m_\ell}{\sqrt{q^2}}\mathrm{Re}(A_0^L A_S^* + A_0^{R*} A_S),$$

$$J_7 = \sqrt{2}\beta_\ell\left[\mathrm{Im}(A_0^L A_\parallel^{L*} - A_0^R A_\parallel^{R*}) + \frac{m_\ell}{\sqrt{q^2}}\mathrm{Im}(A_\perp^L A_S^* - A_\perp^{R*} A_S)\right],$$

$$J_8 = \frac{1}{\sqrt{2}}\beta_\ell^2\left[\mathrm{Im}(A_0^L A_\perp^{L*} + A_0^R A_\perp^{R*})\right], \qquad J_9 = \beta_\ell^2\left[\mathrm{Im}(A_\parallel^{L*} A_\perp^L + A_\parallel^{R*} A_\perp^R)\right],$$

Link to effective operators

⇛ So here is where the magic happens. At leading order the amplitudes can be written as:

$$A_{\perp}^{L,R} = \sqrt{2}Nm_B(1-\hat{s})\left[(\mathcal{C}_9^{\text{eff}}+\mathcal{C}_9^{\text{eff}\prime})\mp(\mathcal{C}_{10}+\mathcal{C}_{10}')+\frac{2\hat{m}_b}{\hat{s}}(\mathcal{C}_7^{\text{eff}}+\mathcal{C}_7^{\text{eff}\prime})\right]\xi_{\perp}(E_{K^*})$$

$$A_{\parallel}^{L,R} = -\sqrt{2}Nm_B(1-\hat{s})\left[(\mathcal{C}_9^{\text{eff}}-\mathcal{C}_9^{\text{eff}\prime})\mp(\mathcal{C}_{10}-\mathcal{C}_{10}')+\frac{2\hat{m}_b}{\hat{s}}(\mathcal{C}_7^{\text{eff}}-\mathcal{C}_7^{\text{eff}\prime})\right]\xi_{\perp}(E_{K^*})$$

$$A_{0}^{L,R} = -\frac{Nm_B(1-\hat{s})^2}{2\hat{m}_{K^*}\sqrt{\hat{s}}}\left[(\mathcal{C}_9^{\text{eff}}-\mathcal{C}_9^{\text{eff}\prime})\mp(\mathcal{C}_{10}-\mathcal{C}_{10}')+2\hat{m}_b(\mathcal{C}_7^{\text{eff}}-\mathcal{C}_7^{\text{eff}\prime})\right]\xi_{\parallel}(E_{K^*}),$$

where $\hat{s}=q^2/m_B^2$, $\hat{m}_i=m_i/m_B$. The $\xi_{\parallel,\perp}$ are the form factors.

⇛ In practice one measures normalized J by branching fractions:

$$S_i/A_i = \frac{J_i \pm \overline{J}_i}{d\Gamma + d\overline{\Gamma}/dq^2}$$

Link to effective operators

$\Rightarrow$ So here is where the magic happens. At leading order the amplitudes can be written as:

$$A_{\perp}^{L,R} = \sqrt{2}Nm_B(1-\hat{s})\left[(\mathcal{C}_9^{\text{eff}}+\mathcal{C}_9^{\text{eff}\prime})\mp(\mathcal{C}_{10}+\mathcal{C}_{10}')+\frac{2\hat{m}_b}{\hat{s}}(\mathcal{C}_7^{\text{eff}}+\mathcal{C}_7^{\text{eff}\prime})\right]\xi_{\perp}(E_{K^*})$$

$$A_{\parallel}^{L,R} = -\sqrt{2}Nm_B(1-\hat{s})\left[(\mathcal{C}_9^{\text{eff}}-\mathcal{C}_9^{\text{eff}\prime})\mp(\mathcal{C}_{10}-\mathcal{C}_{10}')+\frac{2\hat{m}_b}{\hat{s}}(\mathcal{C}_7^{\text{eff}}-\mathcal{C}_7^{\text{eff}\prime})\right]\xi_{\perp}(E_{K^*})$$

$$A_{0}^{L,R} = -\frac{Nm_B(1-\hat{s})^2}{2\hat{m}_{K^*}\sqrt{\hat{s}}}\left[(\mathcal{C}_9^{\text{eff}}-\mathcal{C}_9^{\text{eff}\prime})\mp(\mathcal{C}_{10}-\mathcal{C}_{10}')+2\hat{m}_b(\mathcal{C}_7^{\text{eff}}-\mathcal{C}_7^{\text{eff}\prime})\right]\xi_{\parallel}(E_{K^*}),$$

where $\hat{s}=q^2/m_B^2$, $\hat{m}_i=m_i/m_B$. The $\xi_{\parallel,\perp}$ are the form factors.

$\Rightarrow$ Now we can construct observables that cancel the ξ form factors at leading order:

$$P_5' = \frac{J_5+\bar{J}_5}{2\sqrt{-(J_2^c+\bar{J}_2^c)(J_2^s+\bar{J}_2^s)}}$$

LHCb measurement of $B_d^0 \to K^* \mu\mu$

LHCbs $B^0 \to K^*\mu^-\mu^+$, Selection

⇛ Trigger

- Muon trigger.
- Topological trigger.

⇛ Good modelling with MC.

⇛ Selection:

- As loose as possible.
- Based on the B^0 vertex quality, impact parameters, loose Particle identification for the hadrons.
- The variables were chosen in a way we are sure the are correctly modelled in MC.

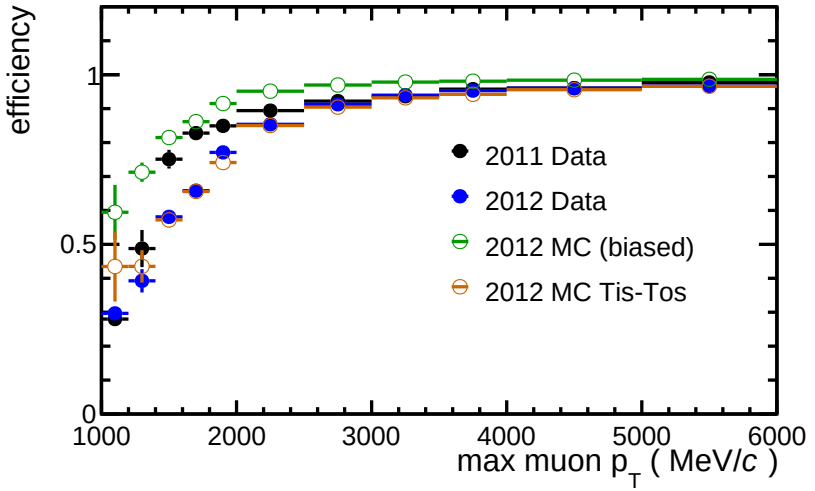

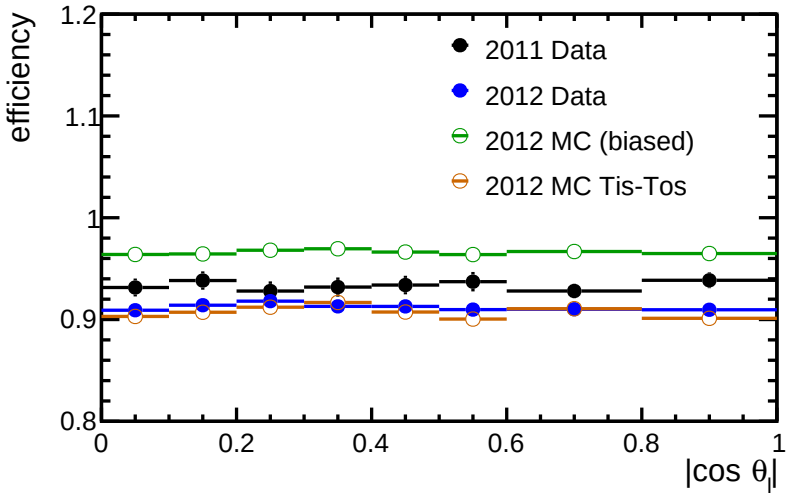

Peaking backgrounds

- ⇛ A number of peaking backgrounds that can mistaken as your signal.
- ⇛ There where a specially designed vetoes to fight each of them.

Channel	after preselection, before vetoes Estimated events	% signal	after vetoes and selection Estimated events	% signal
$\Lambda_b \to \Lambda^*(1520)^0 \mu\mu$	$(1.0 \pm 0.5) \times 10^3$	19 ± 8	51 ± 25	1.0 ± 0.4
$\Lambda_b \to pK\mu\mu$	$(1.0 \pm 0.5) \times 10^2$	1.9 ± 0.8	5.7 ± 2.8	0.11 ± 0.05
$B_d^0 \to K^+\mu\mu$	28 ± 7	0.55 ± 0.06	1.6 ± 0.5	0.031 ± 0.006
$B_s^0 \to \phi\mu\mu$	$(3.2 \pm 1.3) \times 10^2$	6.2 ± 2.1	17 ± 7	0.33 ± 0.12
signal swaps	$(3.6 \pm 0.9) \times 10^2$	6.9 ± 0.6	33 ± 9	0.64 ± 0.06
$B_d^0 \to K^* J/\psi$ swaps	$(1.3 \pm 0.4) \times 10^2$	2.6 ± 0.4	2.7 ± 2.8	0.05 ± 0.05

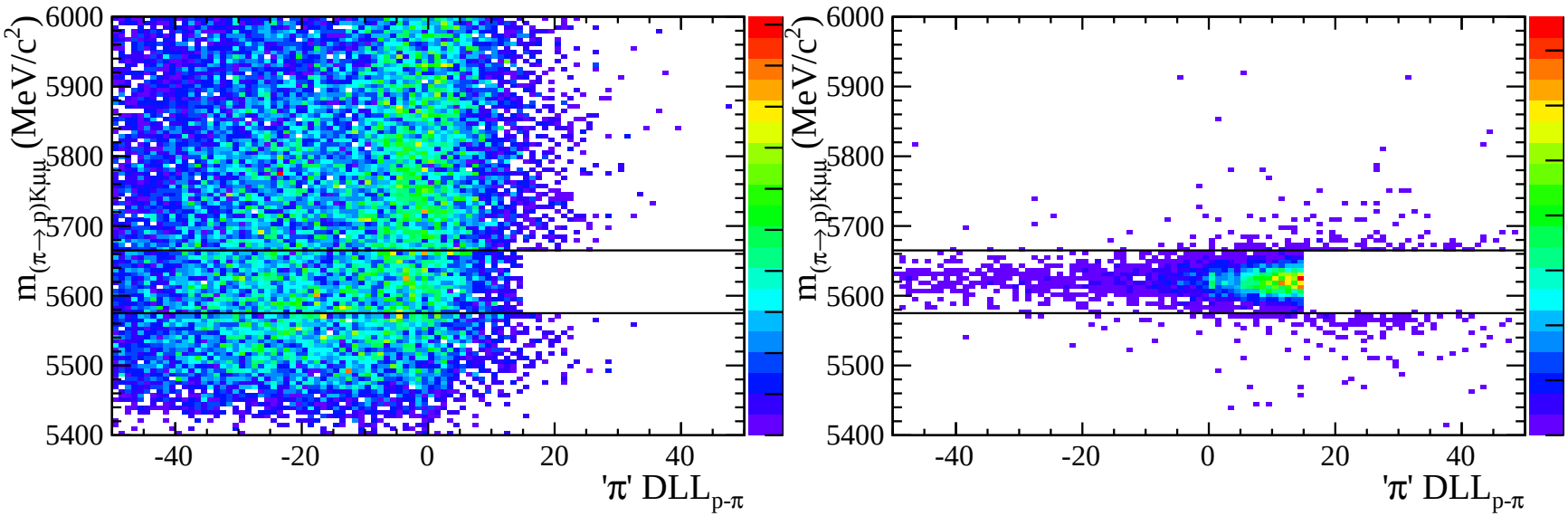

Multivariate simulation

- PID, kinematics and isolation variables used in a Boosted Decision Tree (BDT) to discriminate signal and background.
- BDT with k-Folding technique.
- Completely data driven.

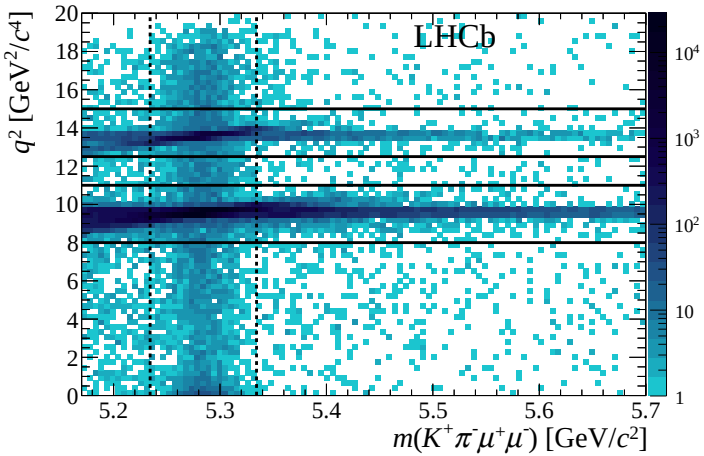

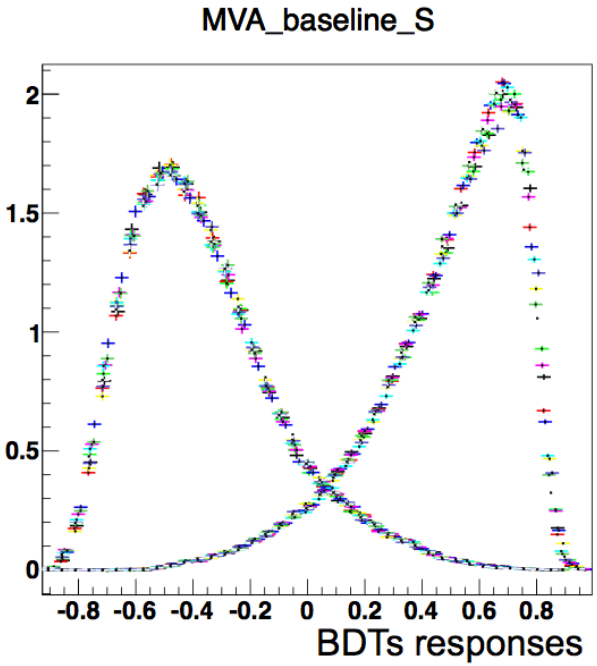

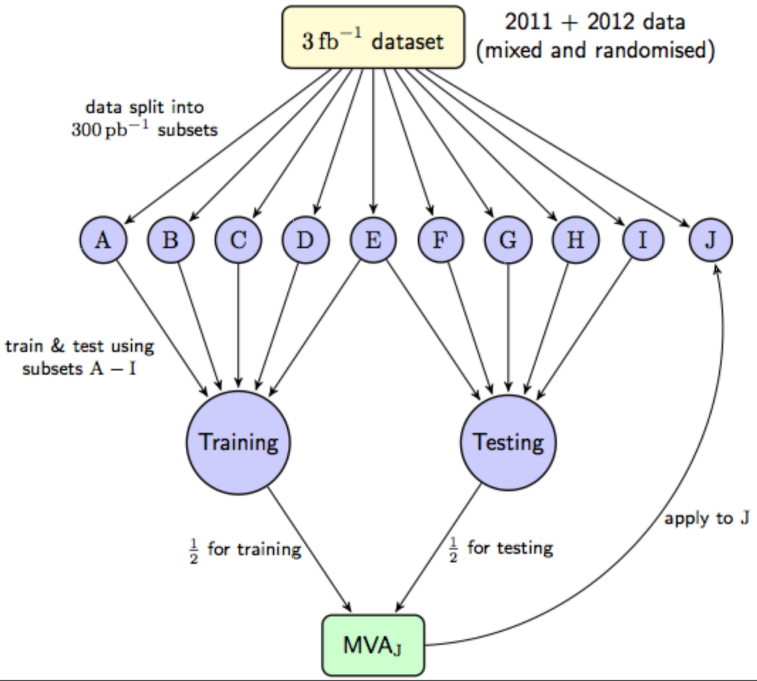

Multivariate simulation, efficiency

⇛ BDT was also checked in order not to bias our angular distribution:

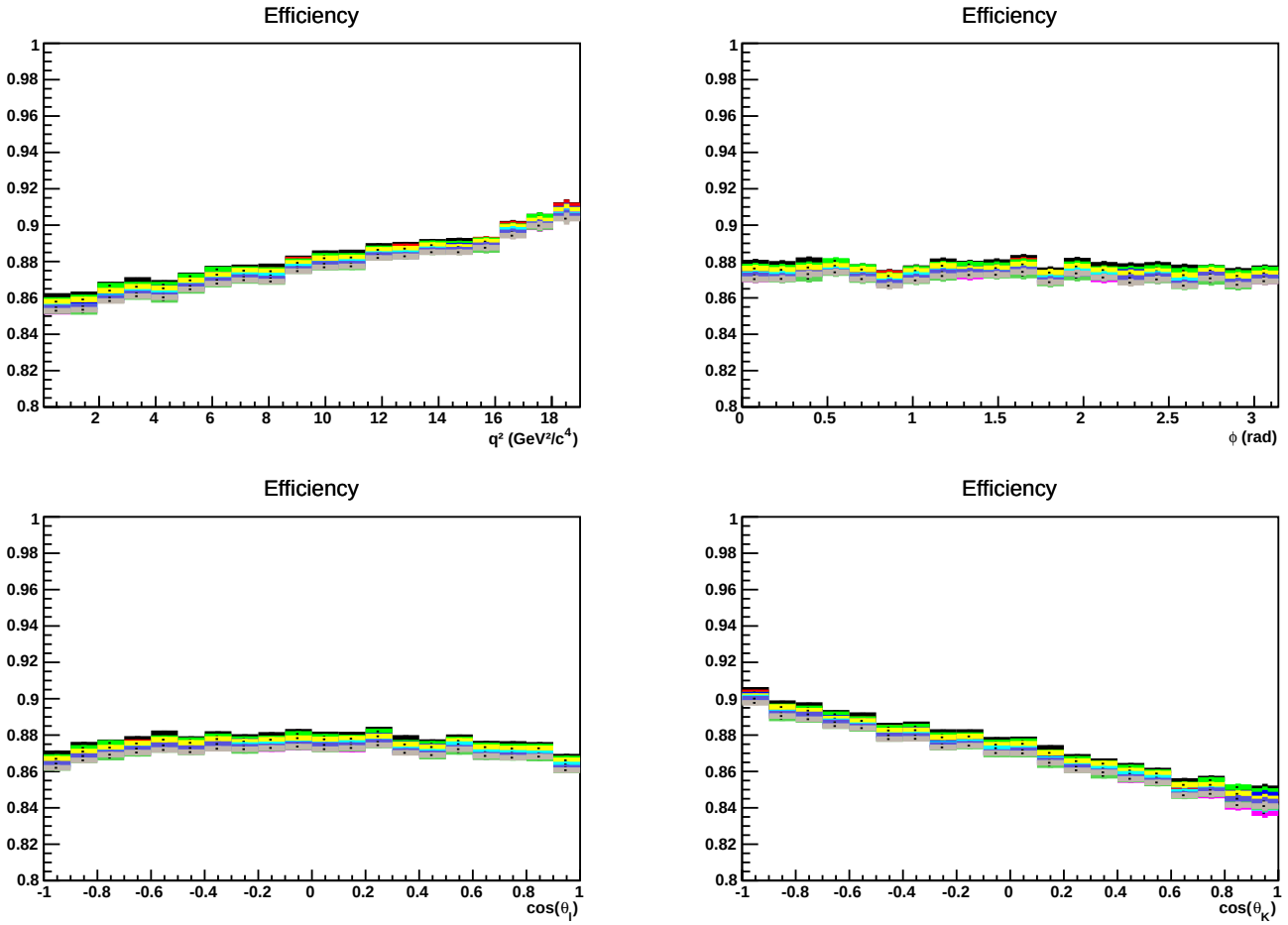

⇛ The BDT has small impact on our angular observables. We will correct for these effects later on.

Mass modelling

⇛ The signal is modelled by a sum of two Crystal-Ball functions with common mean.
⇛ The background is a single exponential.
⇛ The base parameters are obtained from the proxy channel: $B_d^0 \to J/\psi(\mu\mu)K^*$.
⇛ All the parameters are fixed in the signal pdf.
⇛ Scaling factors for resolution are determined from MC.
⇛ In fitting the rare mode only the signal, background yield and the slope of the exponential is left floating.

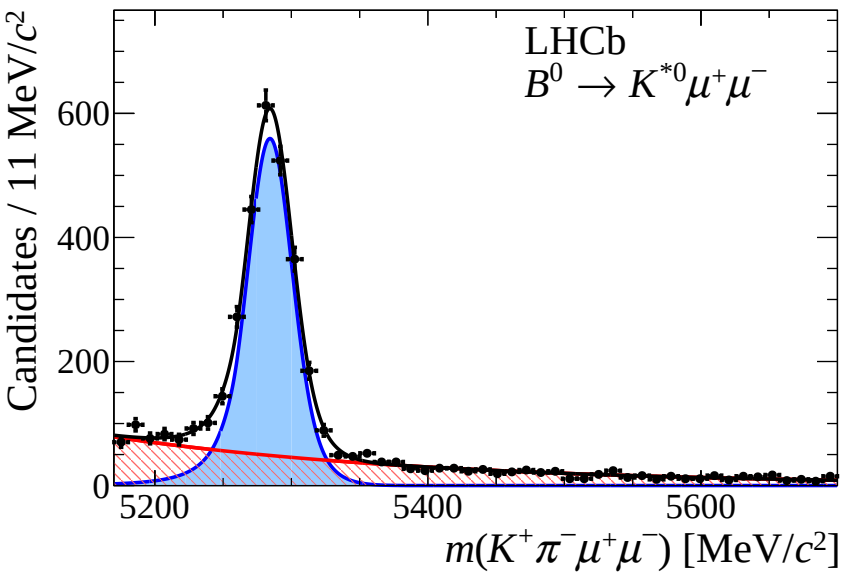

⇛ We found 624 ± 30 candidates in the most interesting $[1.1, 6.0]\ \mathrm{GeV}^2/\mathrm{c}^4$ region
and 2398 ± 57 in the full range $[1.1, 19.]\ \mathrm{GeV}^2/\mathrm{c}^4$.

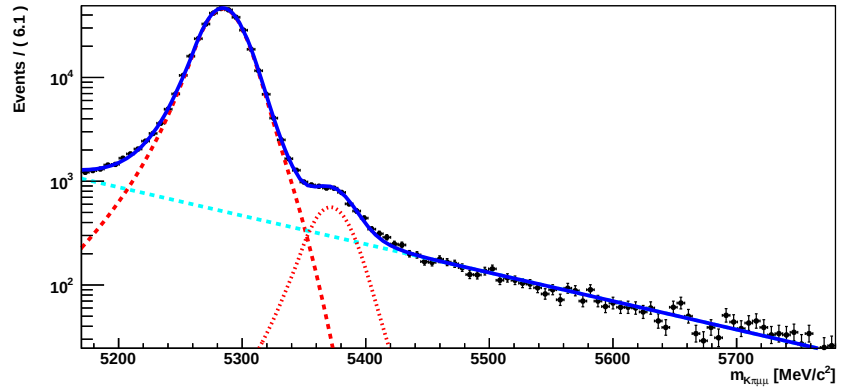

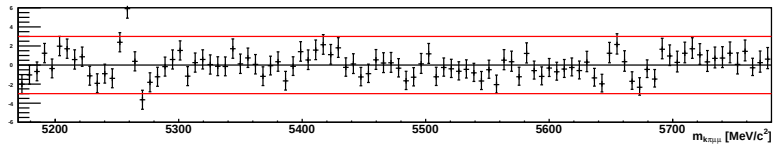

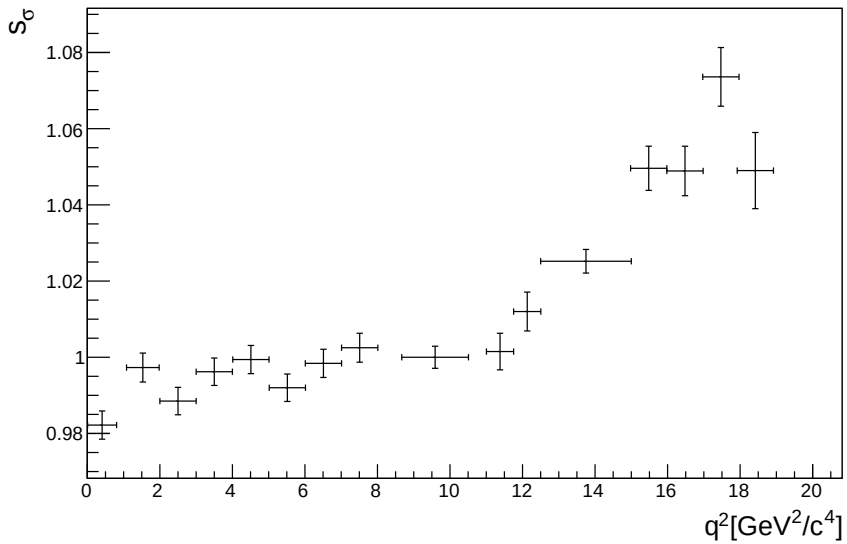

⇛ The S-wave fraction is extracted using a `LASS` model.

Monte Carlo corrections

⇛ No Monte Carlo simulation is perfect! One needs to correct for remaining differences.
⇛ We reweighted our $B_d^0 \to K^*\mu\mu$ Monte Carlo accordingly to differences between the $B_d^0 \to K^*J/\psi$ in data (Splot) and Monte Carlo.

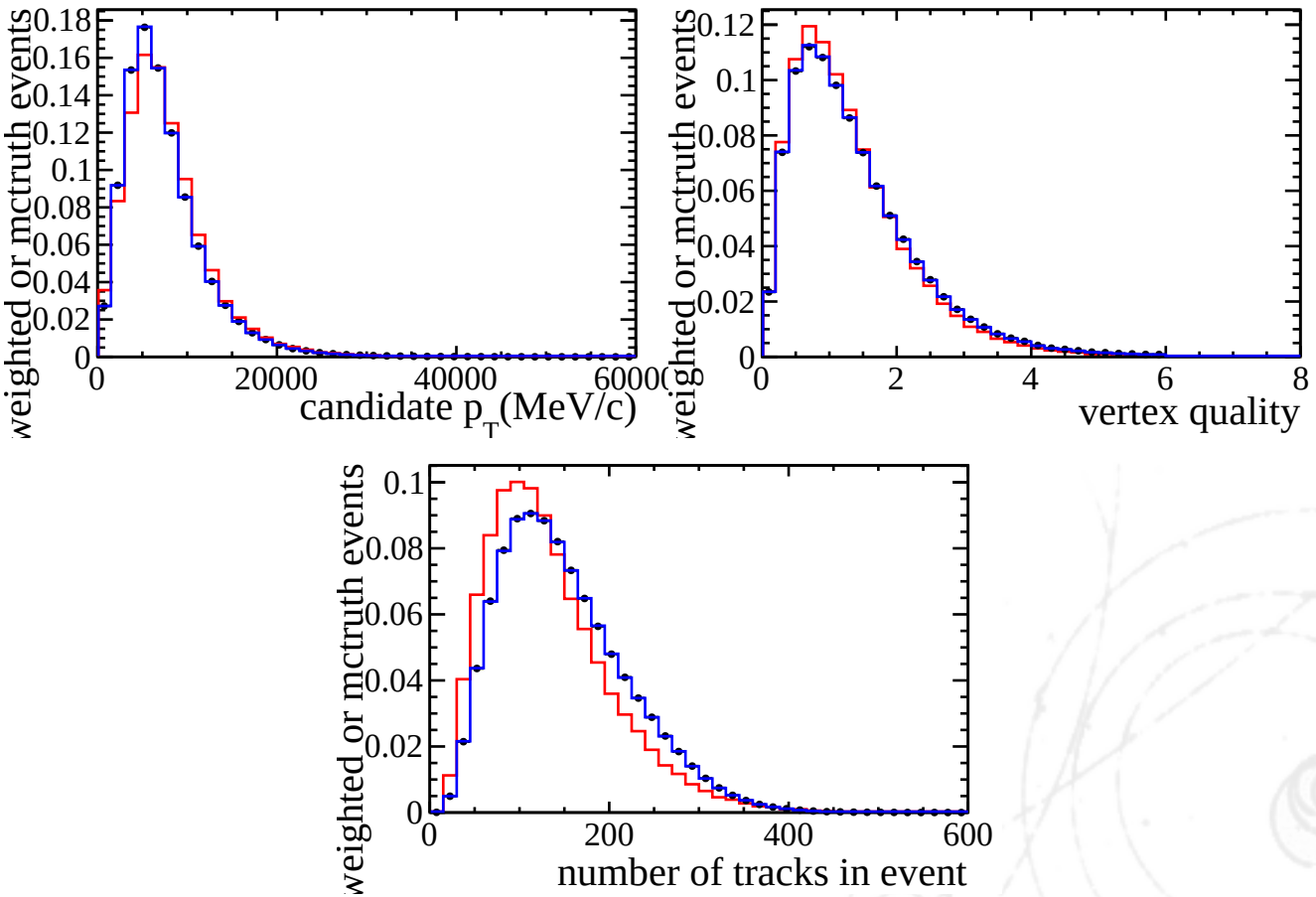

Monte Carlo corrections

⇛ No Monte Carlo simulation is perfect! One needs to correct for remaining differences.
⇛ We reweighted our $B_d^0 \to K^*\mu\mu$ Monte Carlo accordingly to differences between the $B_d^0 \to K^*J/\psi$ in data (Splot) and Monte Carlo.

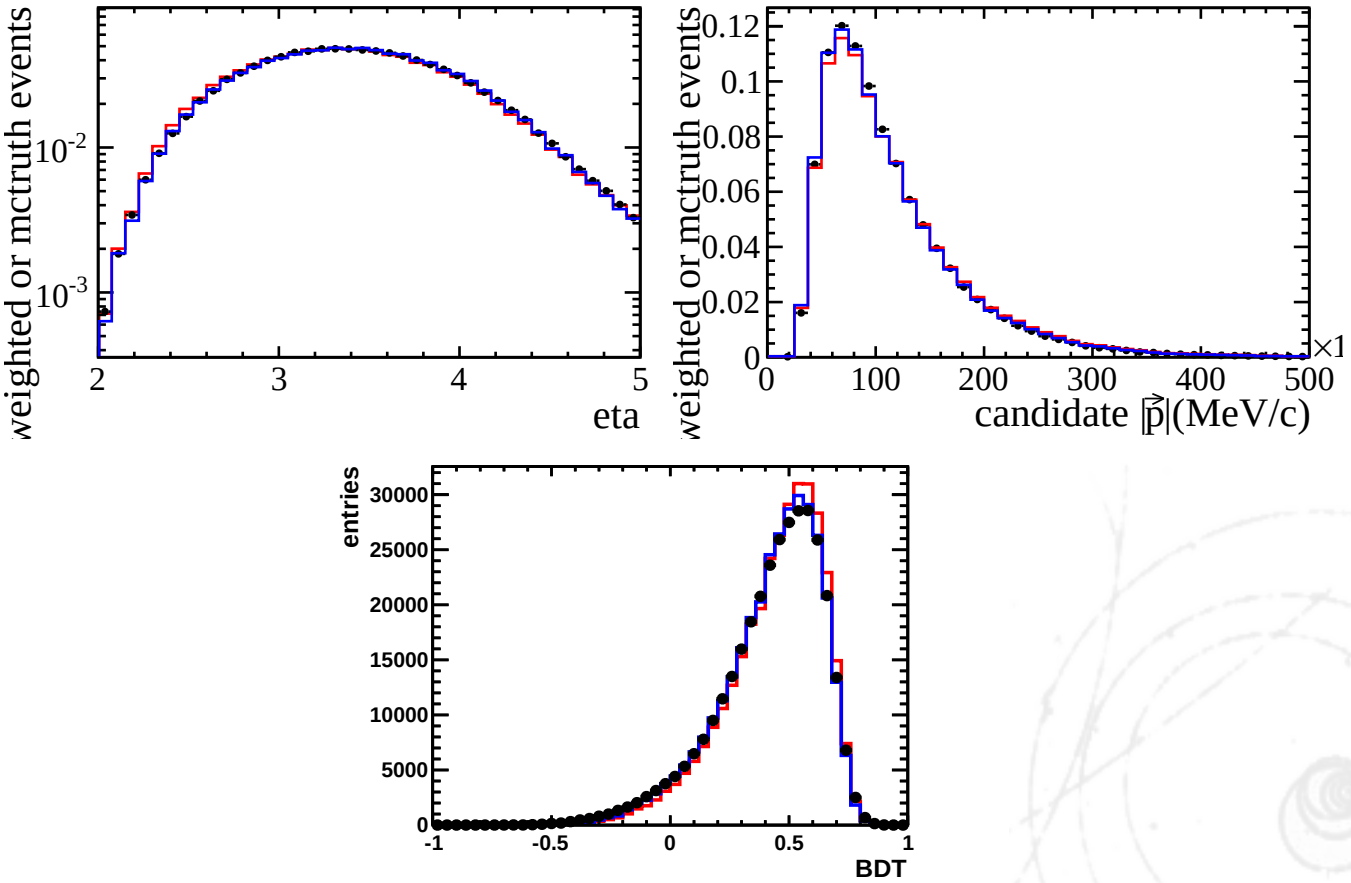

Detector acceptance

- Detector distorts our angular distribution.
- We need to model this effect.
- 4D function is used:

$$\epsilon(\cos\theta_l, \cos\theta_k, \phi, q^2) = \sum_{ijkl} P_i(\cos\theta_l) P_j(\cos\theta_k) P_k(\phi) P_l(q^2),$$

  where P_i is the Legendre polynomial of order i.
- We use up to $4^{th}, 5^{th}, 6^{th}, 5^{th}$ order for the $\cos\theta_l, \cos\theta_k, \phi, q^2$.
- The coefficients were determined using Method of Moments, with a huge simulation sample.
- The simulation was done assuming a flat phase space and reweighing the q^2 distribution to make is flat.
- To make this work the q^2 distribution needs to be reweighted to be flat.

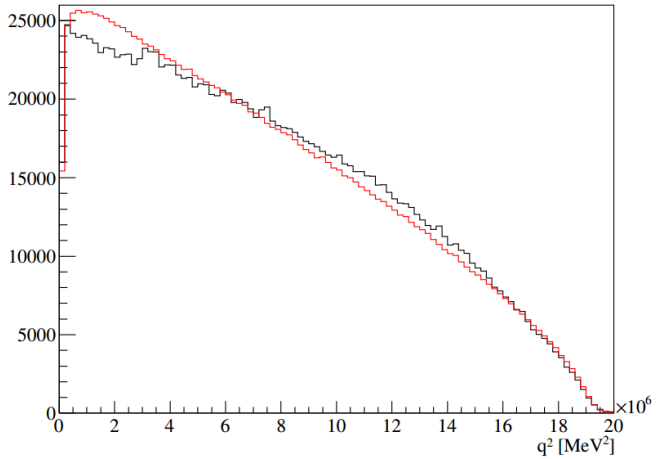

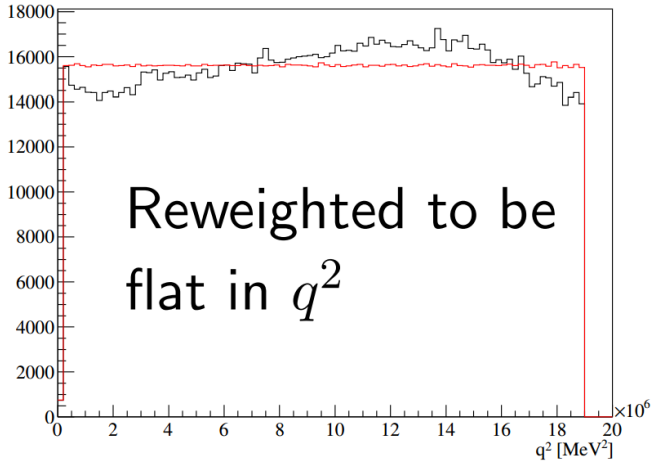

Detector acceptance

- Detector distorts our angular distribution.
- We need to model this effect.
- 4D function is used:

$$\epsilon(\cos\theta_l, \cos\theta_k, \phi, q^2) = \sum_{ijkl} P_i(\cos\theta_l) P_j(\cos\theta_k) P_k(\phi) P_l(q^2),$$

  where P_i is the Legendre polynomial of order i.
- We use up to $4^{th}, 5^{th}, 6^{th}, 5^{th}$ order for the $\cos\theta_l, \cos\theta_k, \phi, q^2$.
- The coefficients were determined using Method of Moments, with a huge simulation sample.
- The simulation was done assuming a flat phase space and reweighing the q^2 distribution to make is flat.
- To make this work the q^2 distribution needs to be reweighted to be flat.

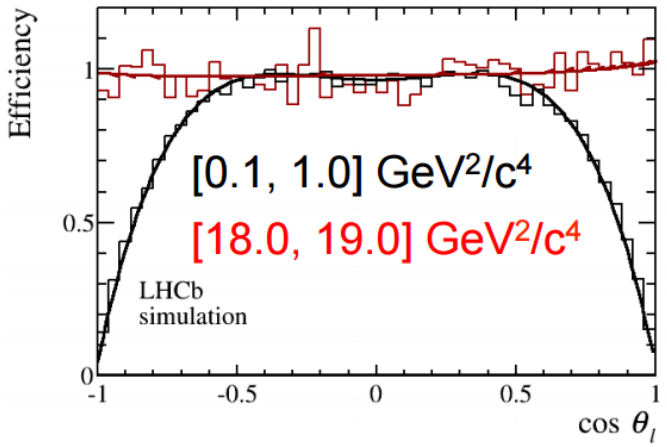

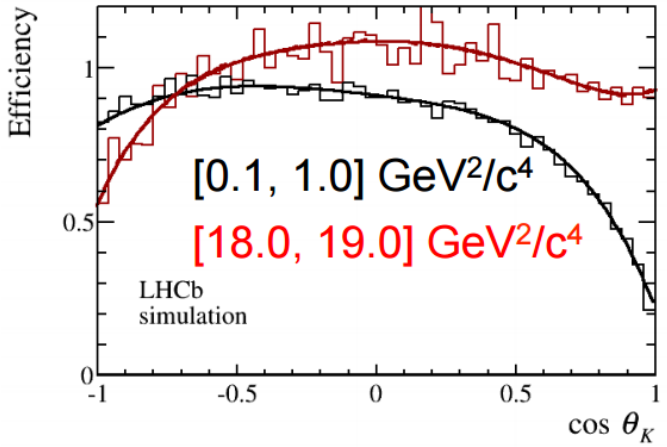

Control channel

- We tested our unfolding procedure on $B \to J/\psi K^*$.
- The result is in perfect agreement with other experiments and our different analysis of this decay.

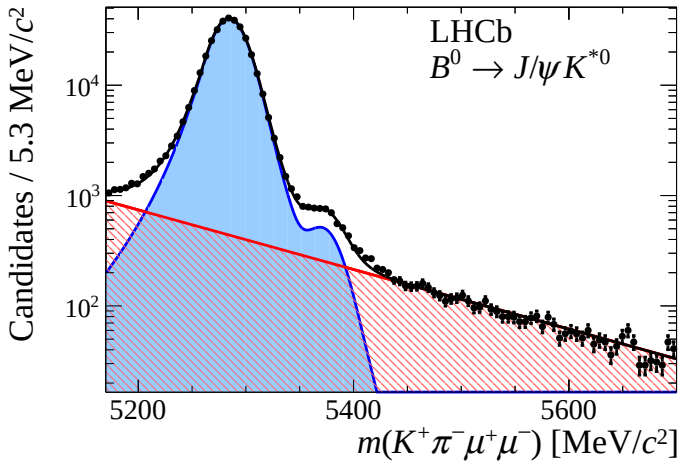

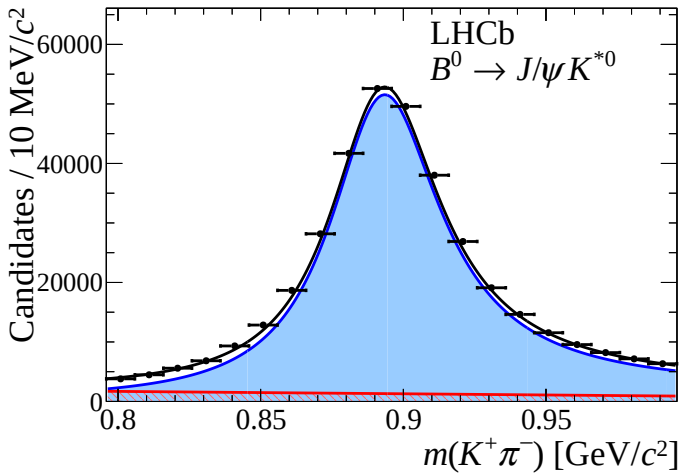

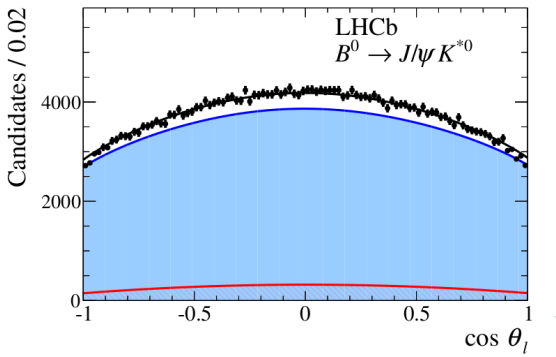

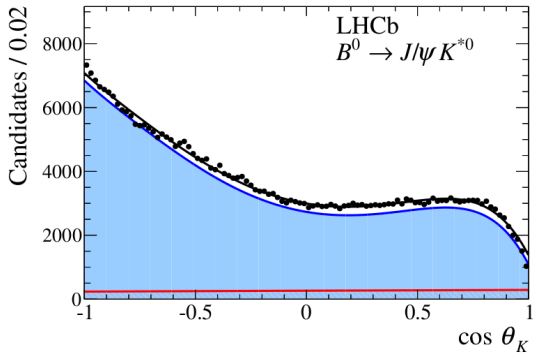

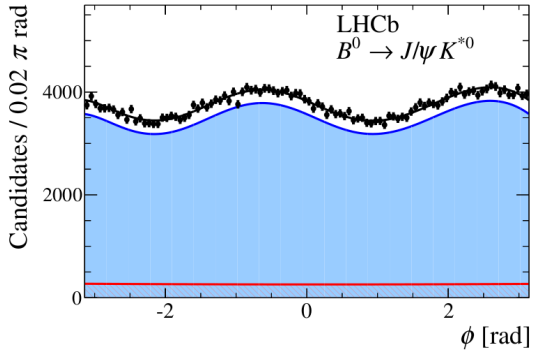

The columns of New Physics

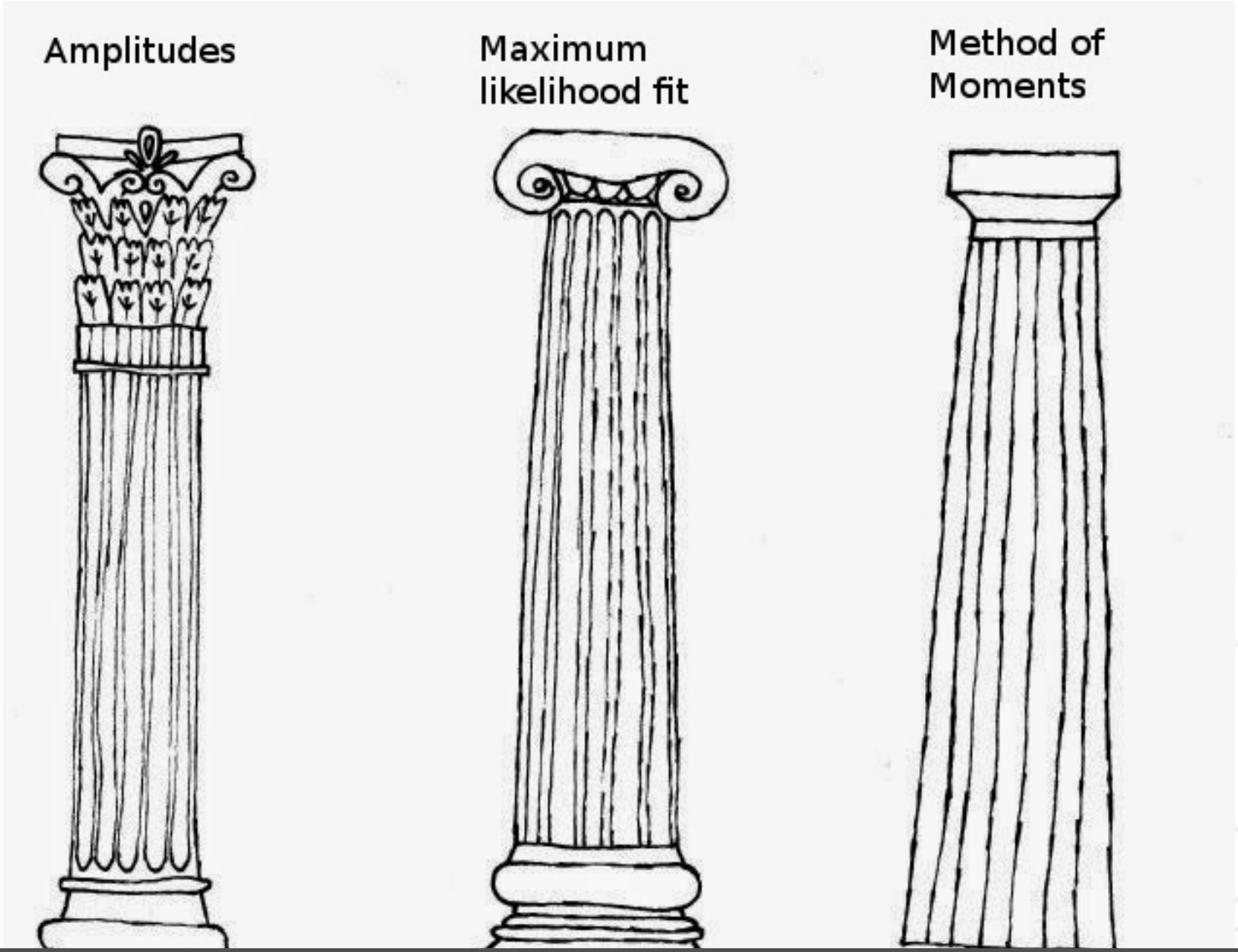

The columns of New Physics

1. Maximum likelihood fit:
   - The most standard way of obtaining the parameters.
   - Suffers from convergence problems, under coverages, etc. in low statistics.
2. Method of moments:
   - Less precise then the likelihood estimator ($10 - 15\%$ larger uncertainties).
   - Does not suffer from the problems of likelihood fit.
3. Amplitude fit:
   - Incorporates all the physical symmetries inside the amplitudes! The most precise estimator.
   - Has theoretical assumptions inside!

Maximum likelihood fit - Results

⇛ In the maximum likelihood fit one could weight the events accordingly to the $\frac{1}{\varepsilon(\cos\theta_l, \cos\theta_k, \phi, q^2)}$

⇛ Better alternative is to put the efficiency into the maximum likelihood fit itself:

$$\mathcal{L} = \prod_{i=1}^{N} \epsilon_i(\Omega_i, q_i^2)\mathcal{P}(\Omega_i, q_i^2) / \int \epsilon(\Omega, q^2)\mathcal{P}(\Omega, q^2) d\Omega dq^2$$

⇛ Only the relative weights matters!

⇛ The Procedure was commissioned with TOY MC study.

⇛ Use Feldmann-Cousins to determine the uncertainties.

⇛ Angular background component is modelled with 2^{nd} order Chebyshev polynomials, which was tested on the side-bands.

⇛ S-wave component treated as nuisance parameter.

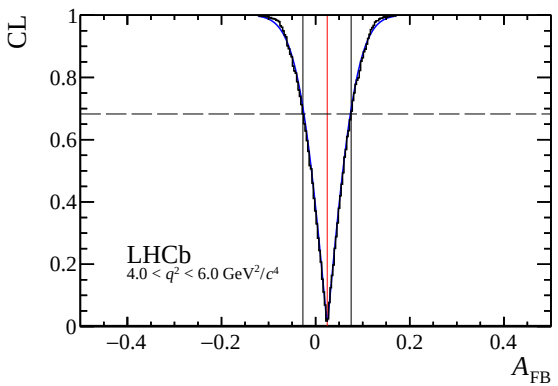

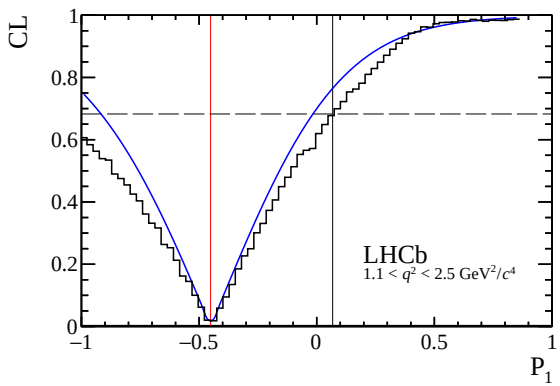

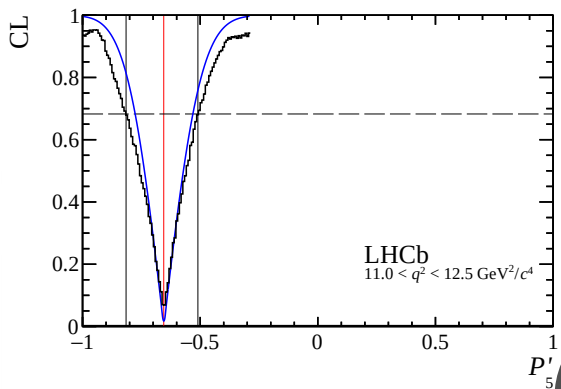

Maximum likelihood fit - Results

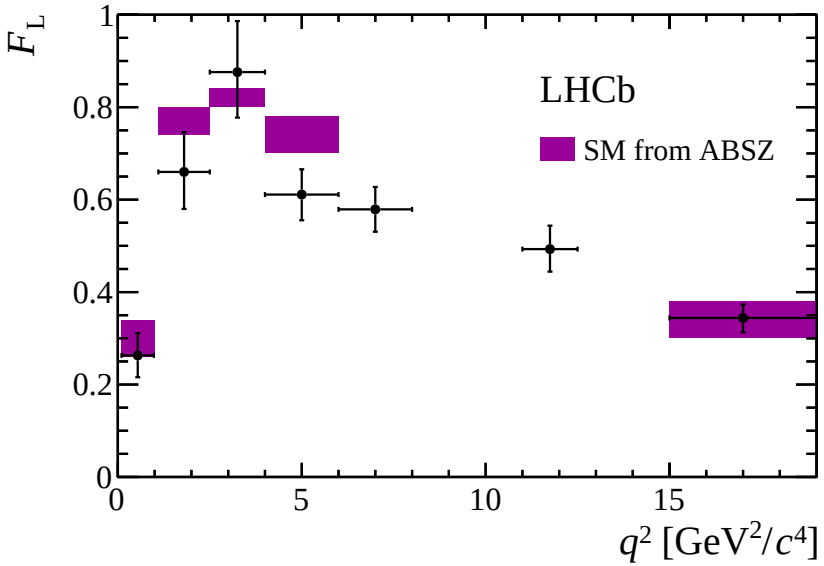

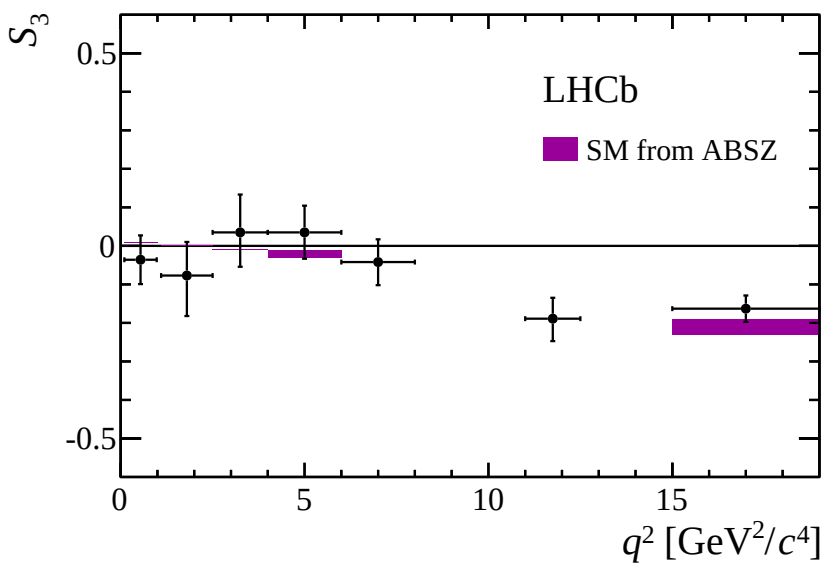

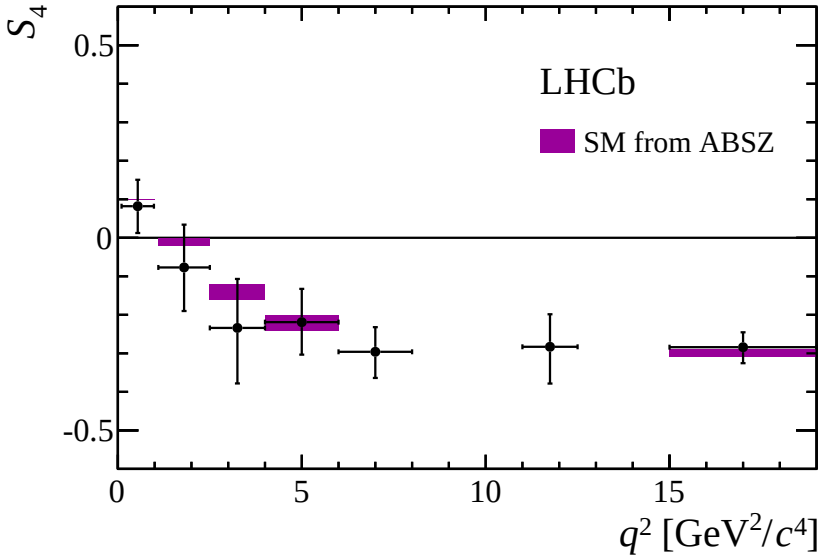

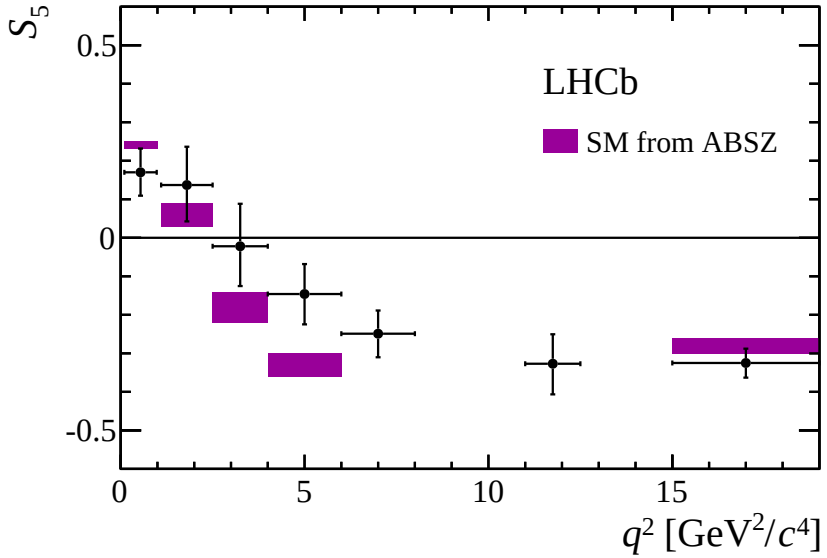

Maximum likelihood fit - Results

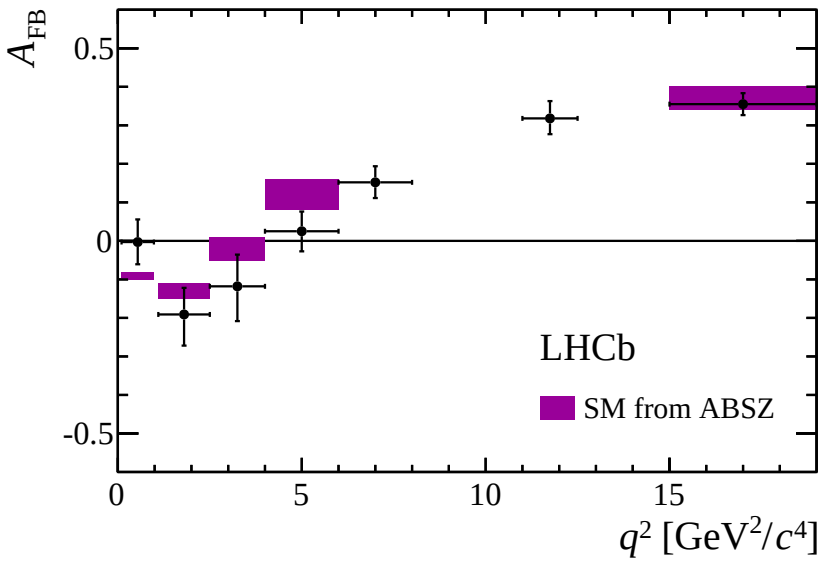

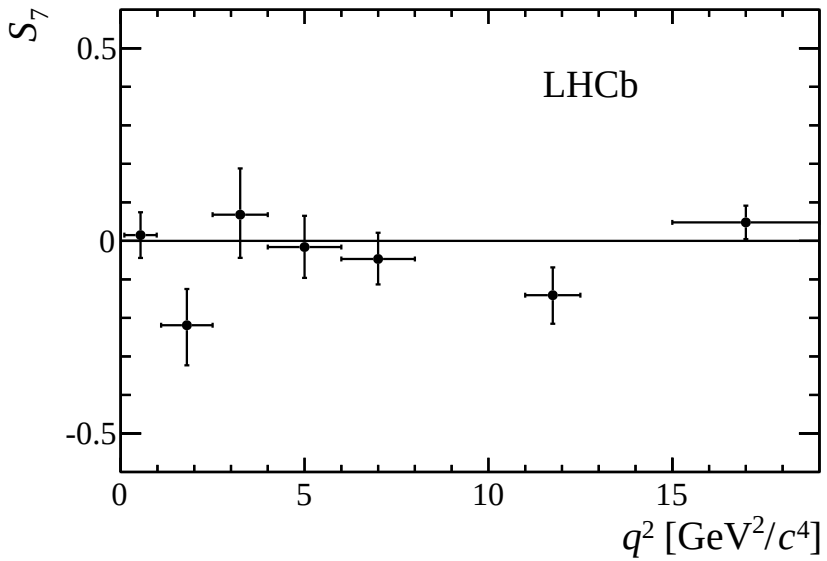

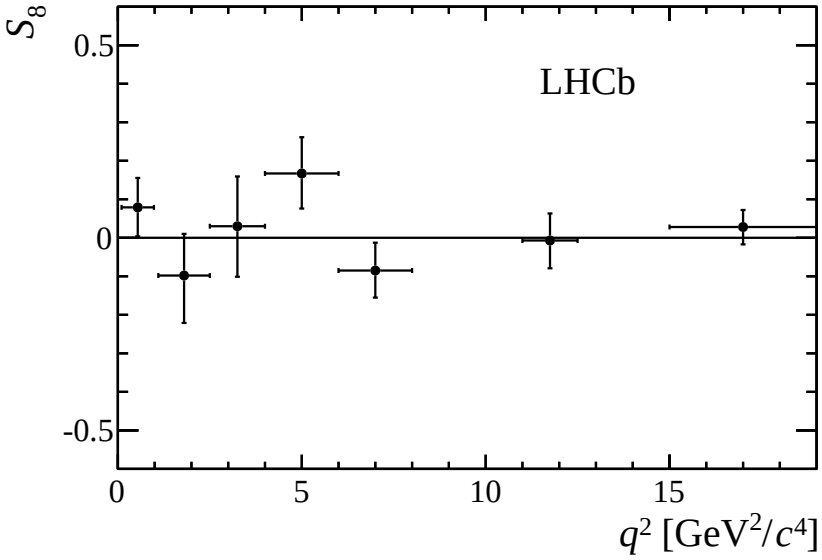

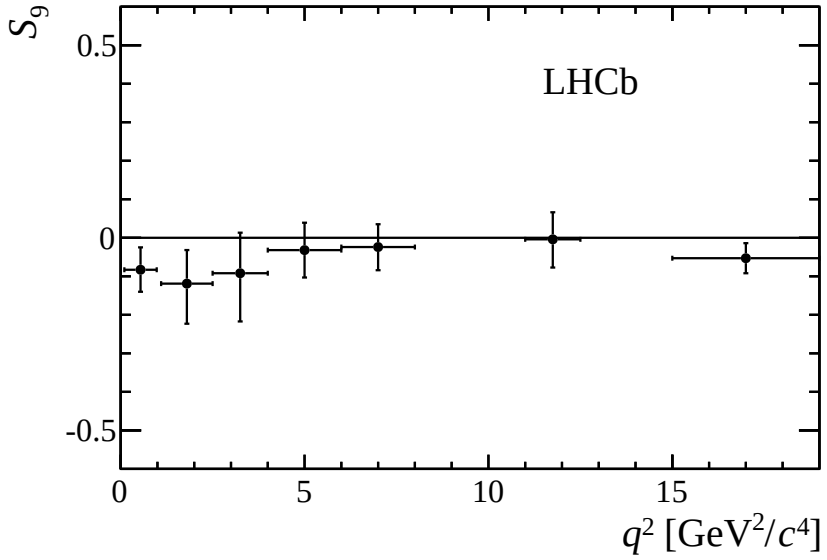

Maximum likelihood fit - Results

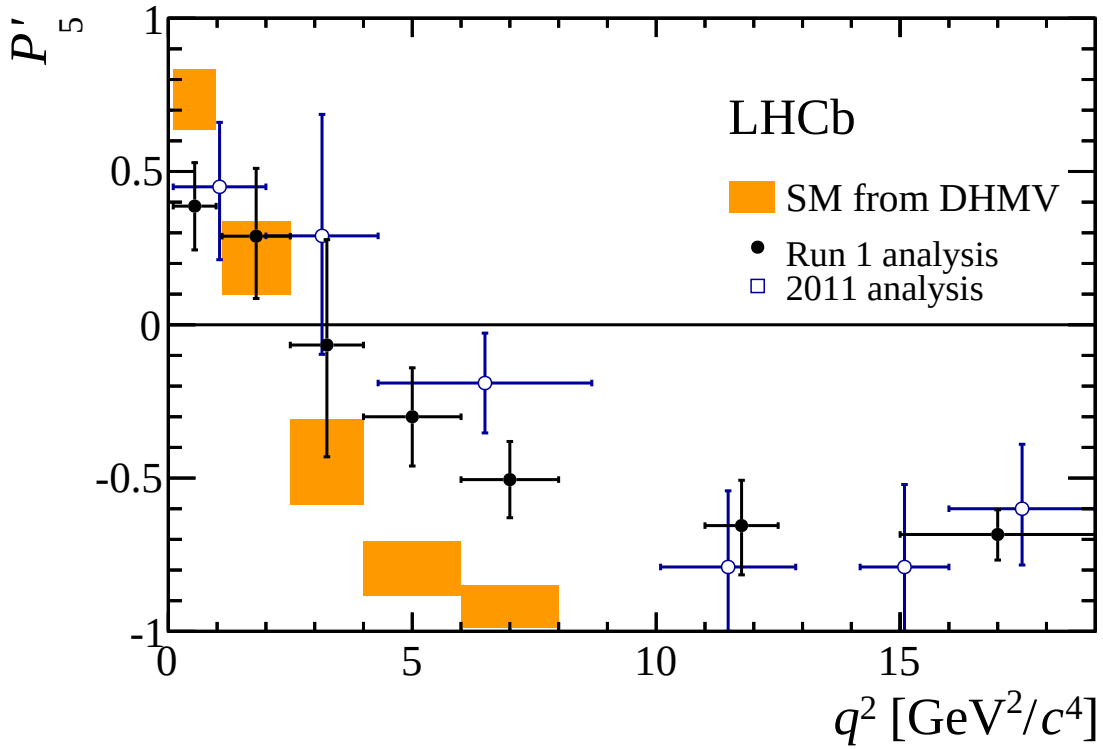

- Tension with $3\ \mathrm{fb}^{-1}$ gets confirmed!
- two bins both deviate by $2.8\ \sigma$ from SM prediction.
- Result compatible with previous result.

Method of moments

⇛ See Phys.Rev.D91(2015)114012, F.Beaujean , M.Chrzaszcz, N.Serra, D. van Dyk for details.

⇛ The idea behind Method of Moments is simple: Use orthogonality of spherical harmonics, $f_j(\overrightarrow{\Omega})$ to solve for coefficients within a q^2 bin:

$$\int f_i(\overrightarrow{\Omega}) f_j(\overrightarrow{\Omega}) = \delta_{ij}$$

$$M_i = \int \left(\frac{1}{d(\Gamma + \bar{\Gamma})/dq^2} \right) \frac{d^3(\Gamma + \bar{\Gamma})}{d\overrightarrow{\Omega}} f_i(\overrightarrow{\Omega}) d\Omega$$

⇛ Don't have true angular distribution but we "sample" it with our data.

⇛ Therefore: $\int \to \sum$ and $M_i \to \widehat{M}_i$

$$\hat{M}_i = \frac{1}{\sum_e \omega_e} \sum_e \omega_e f_i(\overrightarrow{\Omega}_e)$$

⇛ The weight ω accounts for the efficiency. Again the normalization of weights does not matter.

Method of moments - results

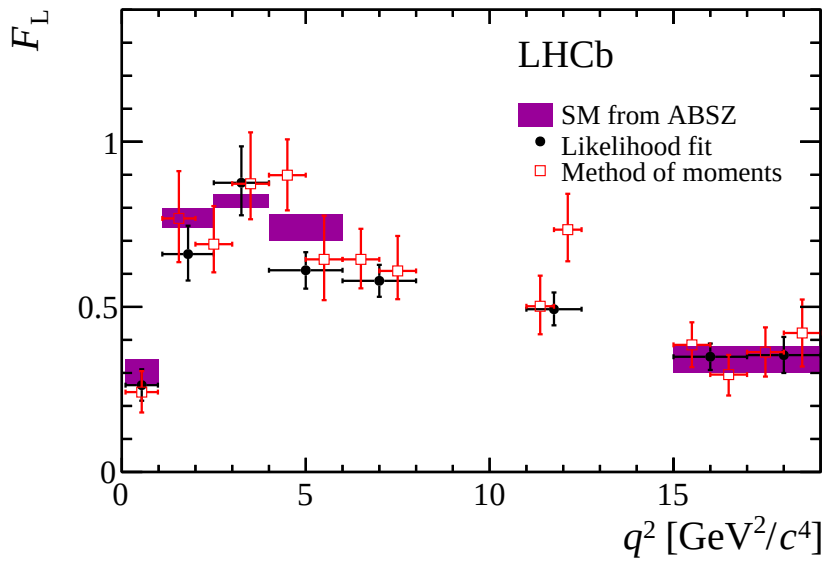

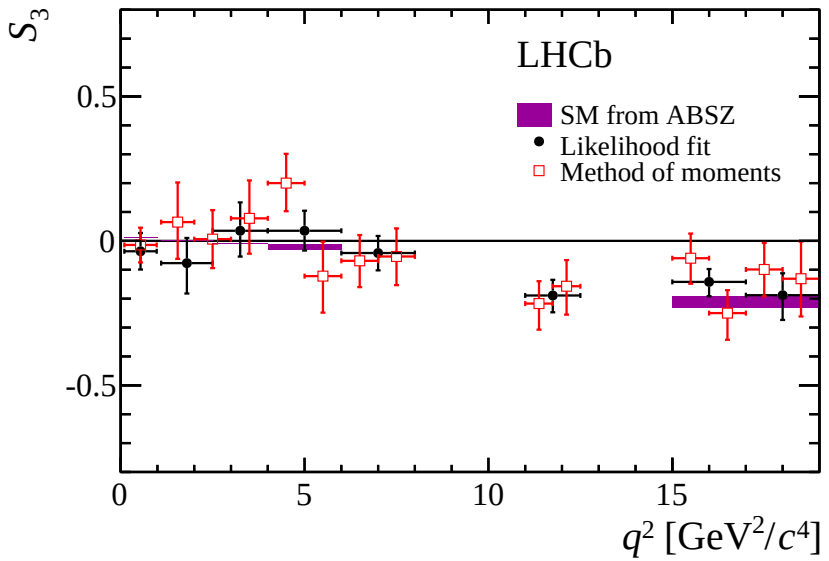

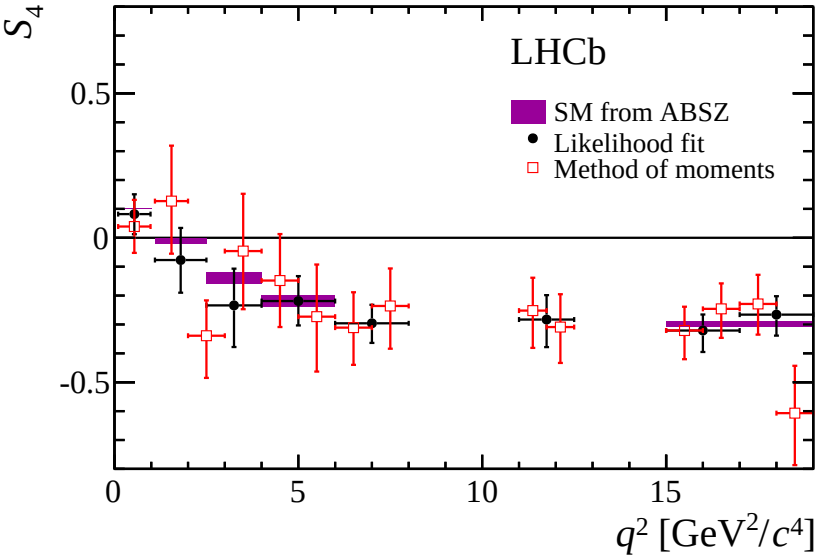

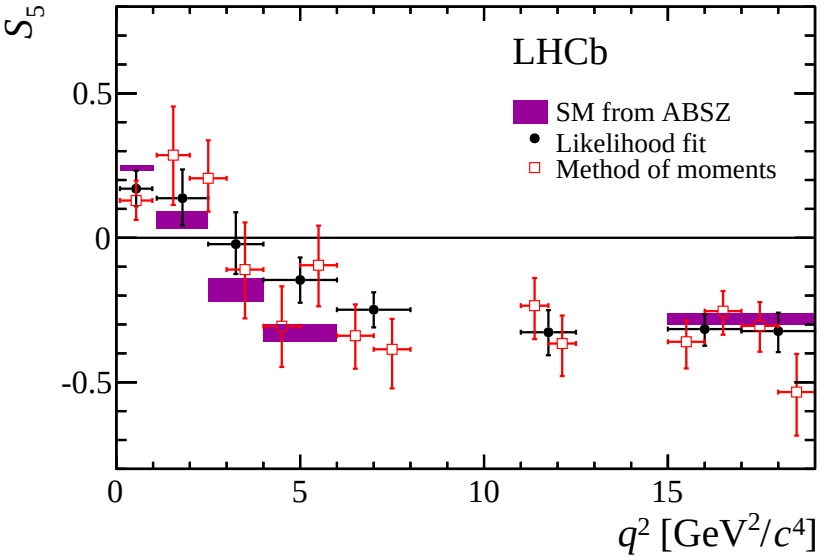

Method of moments - results

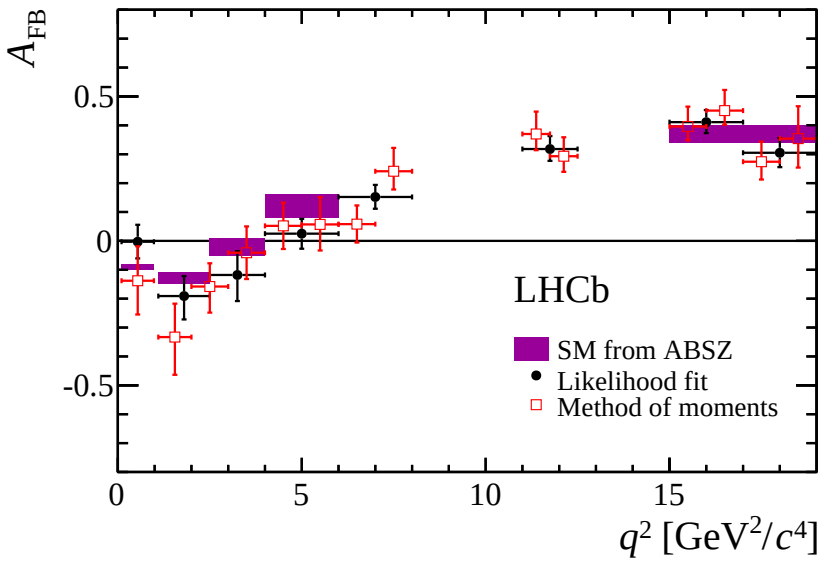

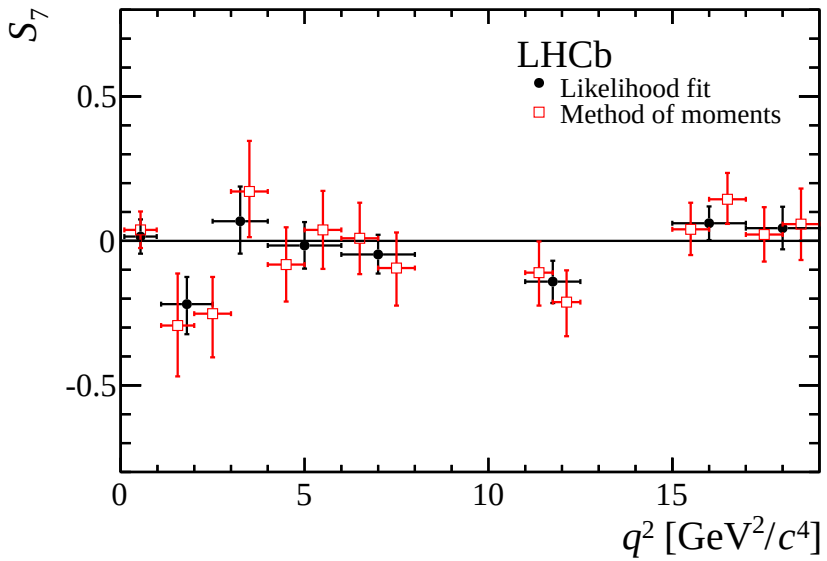

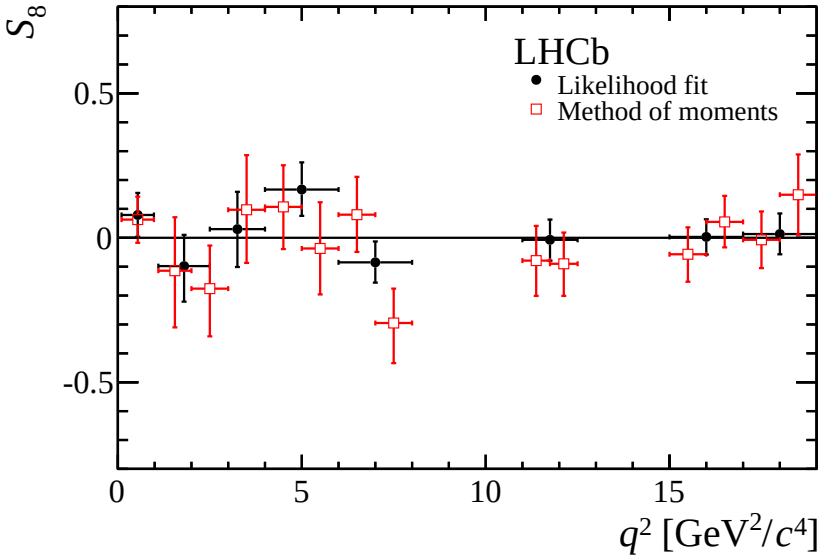

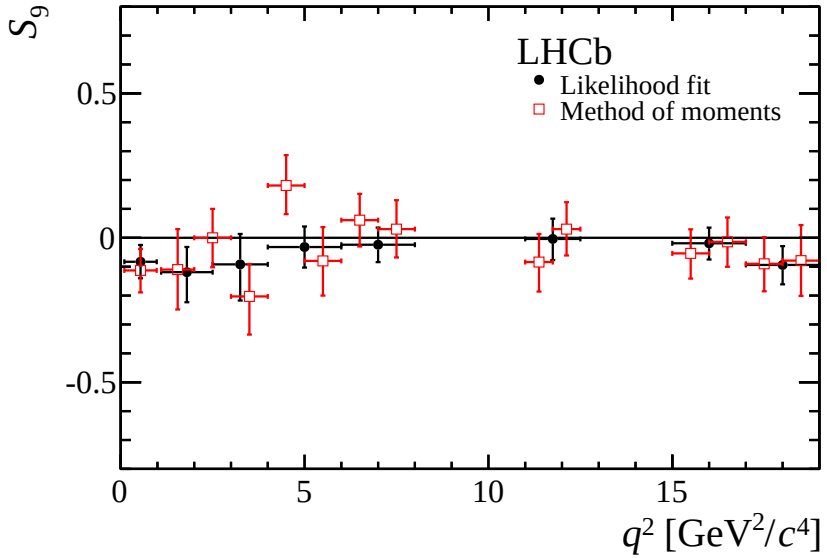

Method of moments - results

⇛ Method of Moments allowed us to measure for the first time a new observable:

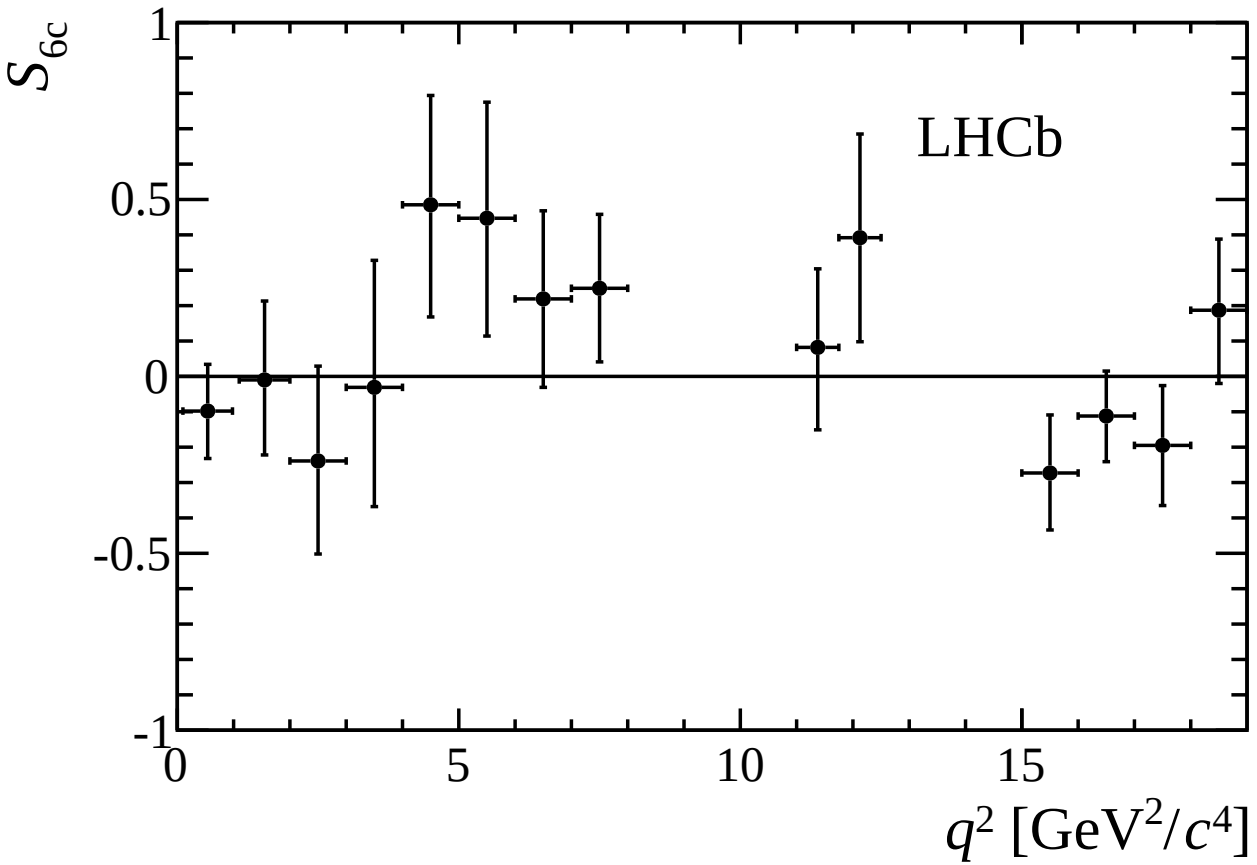

Amplitudes method

$\Rightarrow$ Fit for amplitudes as (continuous) functions of q^2 in the region: $q^2 \in [1.1.6.0]\ \mathrm{GeV}^2/\mathrm{c}^4$.

$\Rightarrow$ Needs some Ansatz:

$$A(q^2) = \alpha + \beta q^2 + \frac{\gamma}{q^2}$$

$\Rightarrow$ The assumption is tested extensively with toys.

$\Rightarrow$ Set of 3 complex parameters α, β, γ per vector amplitude:

- $L,\ R,\ 0,\ \|,\ \perp,\ \Re,\ \Im \rightarrowtail\ \ 3 \times 2 \times 3 \times 2 = 36$ DoF.
- Scalar amplitudes: $+4$ DoF.
- Symmetries of the amplitudes reduces the total budget to: 28.

$\Rightarrow$ The technique is described in JHEP06(2015)084.

$\Rightarrow$ Allows to build the observables as continuous functions of q^2:

- At current point the method is limited by statistics.
- In the future the power of this method will increase.

$\Rightarrow$ Allows to measure the zero-crossing points for free and with smaller errors than previous methods.

Amplitudes - results

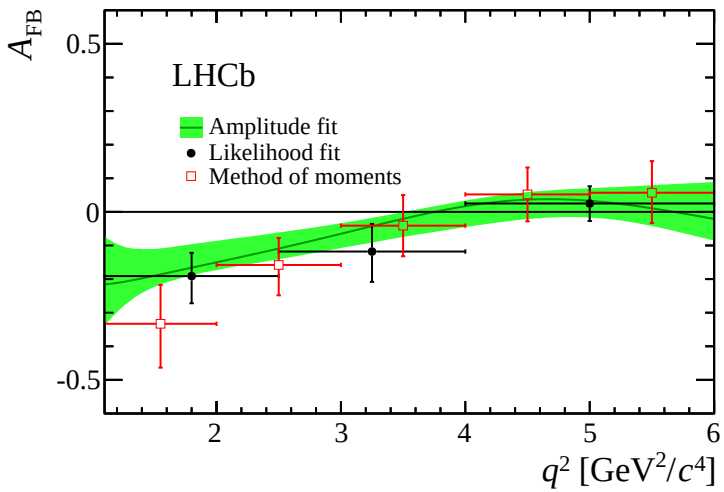

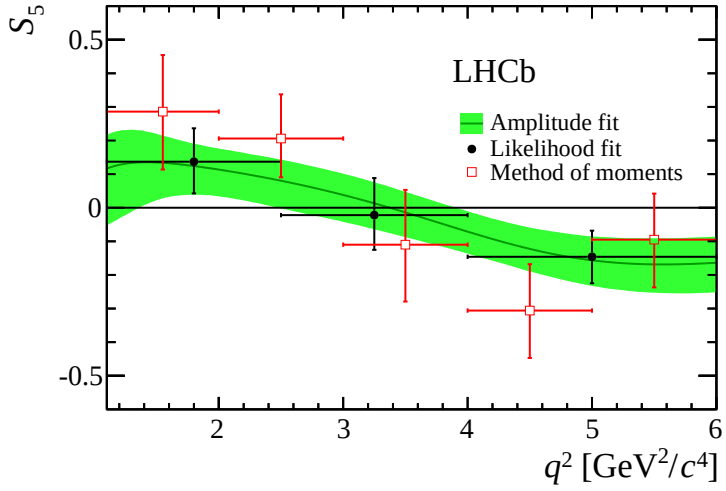

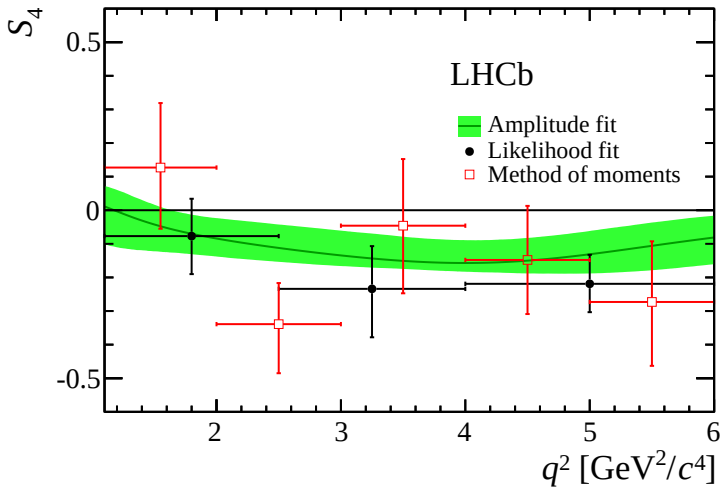

Zero crossing points:

$$q_0(S_4) < 2.65 \quad \text{at } 95\%\ CL$$
$$q_0(S_5) \in [2.49, 3.95] \quad \text{at } 68\%\ CL$$
$$q_0(A_{FB}) \in [3.40, 4.87] \quad \text{at } 68\%\ CL$$

Compatibility with SM

$\Rightarrow$ Use EOS software package to test compatibility with SM.

$\Rightarrow$ Perform the χ^2 fit to the measured:

$$F_L, A_{FB}, S_{3,\ldots,9}.$$

$\Rightarrow$ Float a vector coupling: $\Re(C_9)$.

$\Rightarrow$ Best fit is found to be $3.4\ \sigma$ away from the SM.

$$\Delta\Re(C_9) \equiv \Re(C_9)^{\text{fit}} - \Re(C_9)^{\text{SM}} = -1.03$$

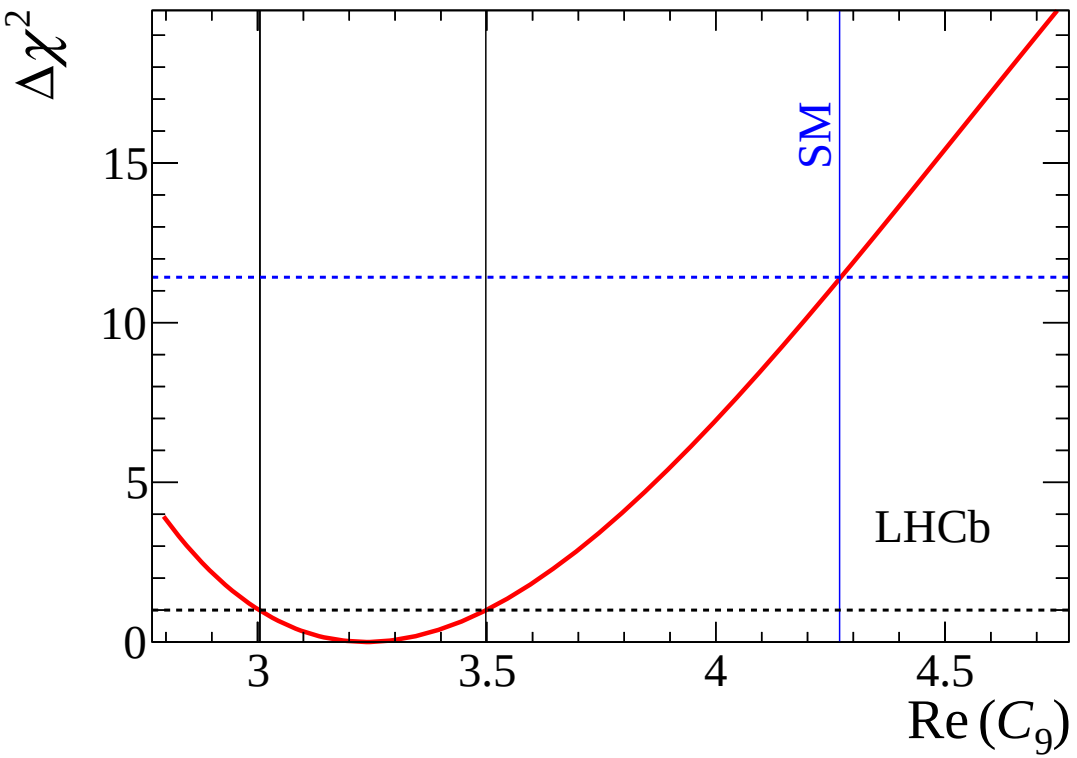

Other related LHCb measurements.

Branching fraction measurements of $B \to K^{*\pm}\mu\mu$

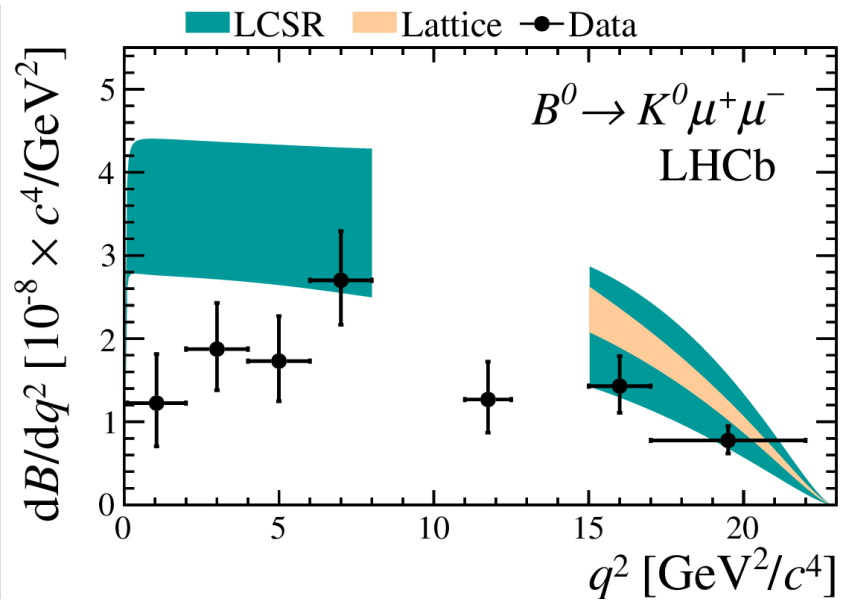

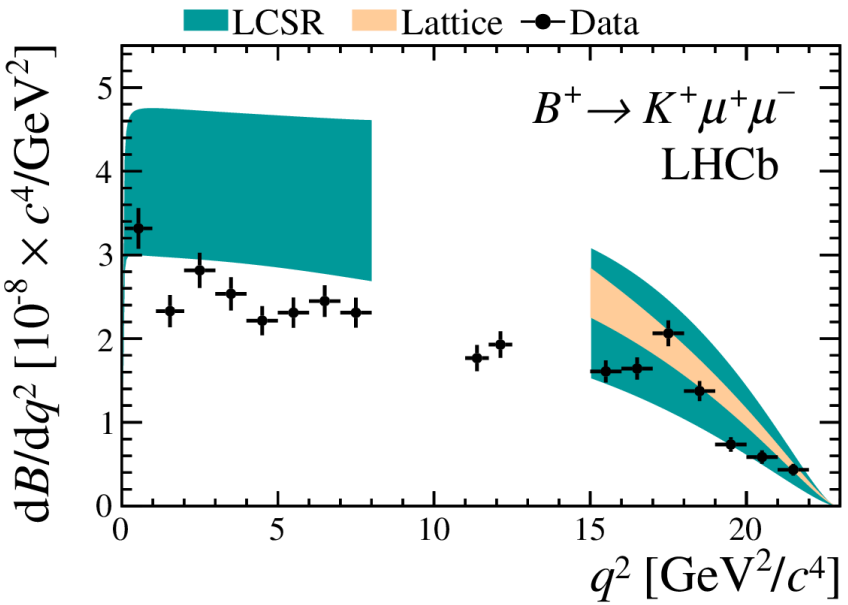

- Despite large theoretical errors the results are consistently smaller than SM prediction.

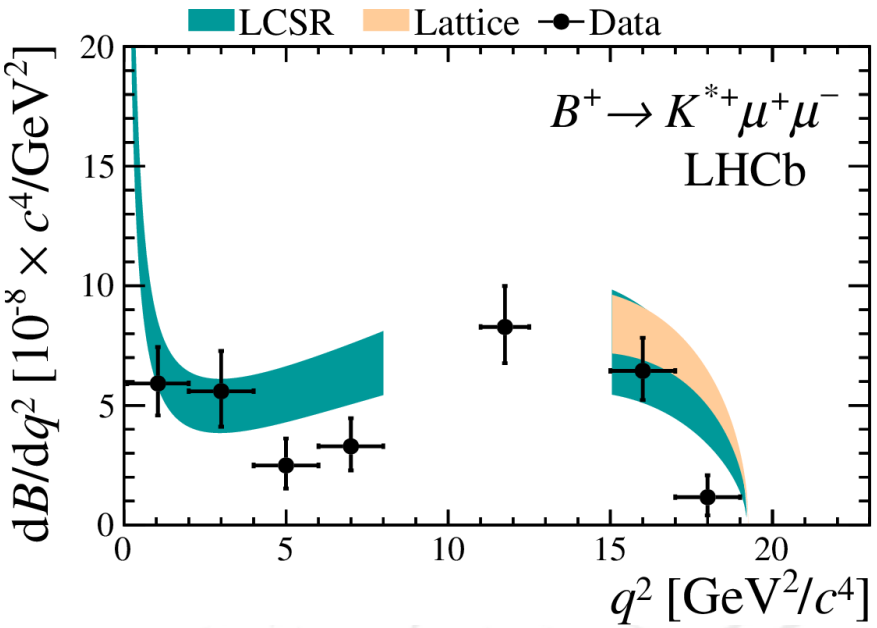

Branching fraction measurements of $B_s^0 \to \phi\mu\mu$

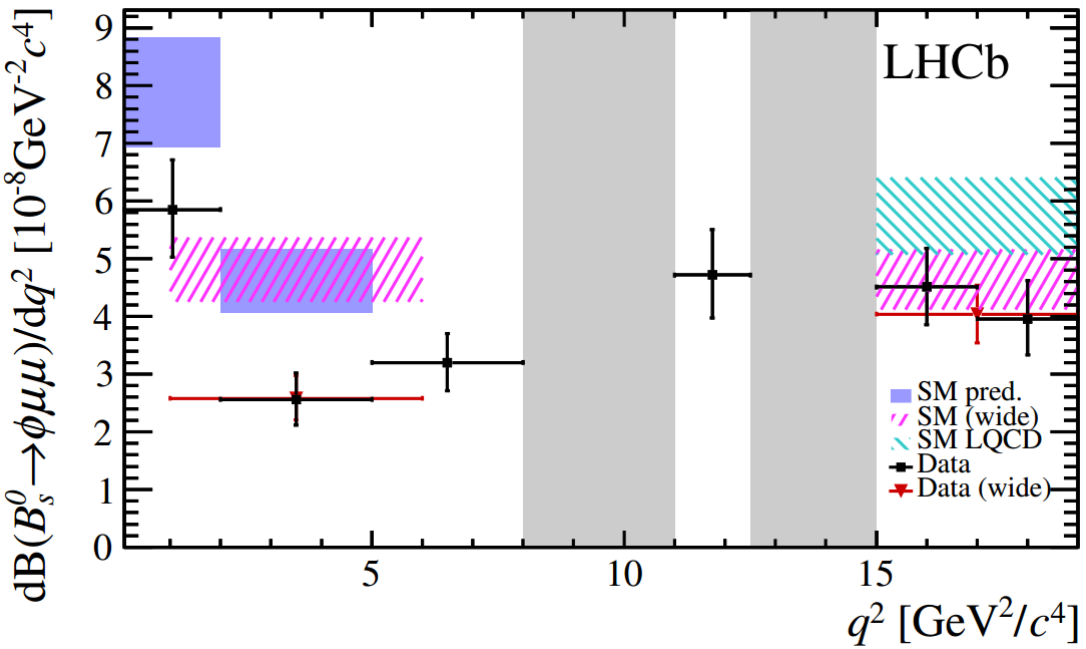

- Recent LHCb measurement [JHEPP09 (2015) 179].
- Suppressed by $\frac{f_s}{f_d}$.
- Cleaner because of narrow ϕ resonance.
- $3.3\ \sigma$ deviation in SM in the $1 - 6\mathrm{GeV}^2$ bin.

Branching fraction measurements of $\Lambda_b \to \Lambda\mu\mu$

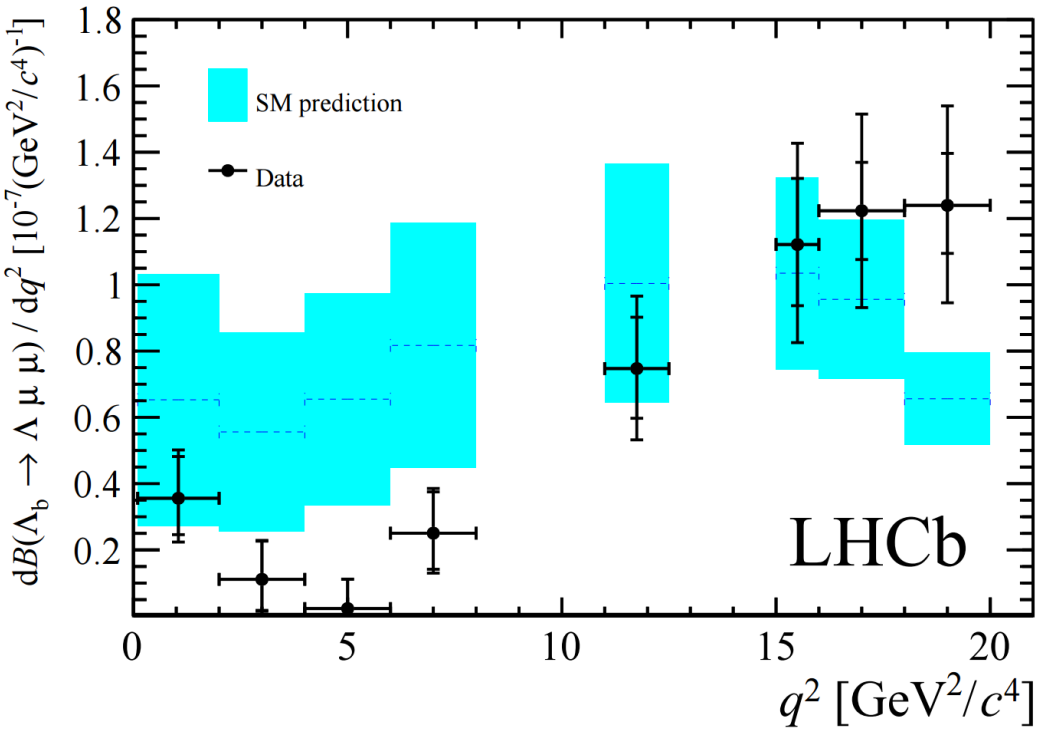

- This years LHCb measurement [JHEP 06 (2015) 115]].
- In total ~ 300 candidates in data set.
- Decay not present in the low q^2.

Branching fraction measurements of $\Lambda_b \to \Lambda\mu\mu$

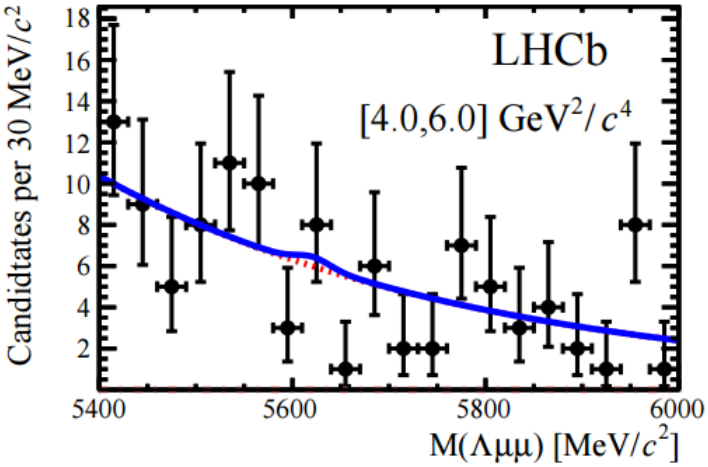

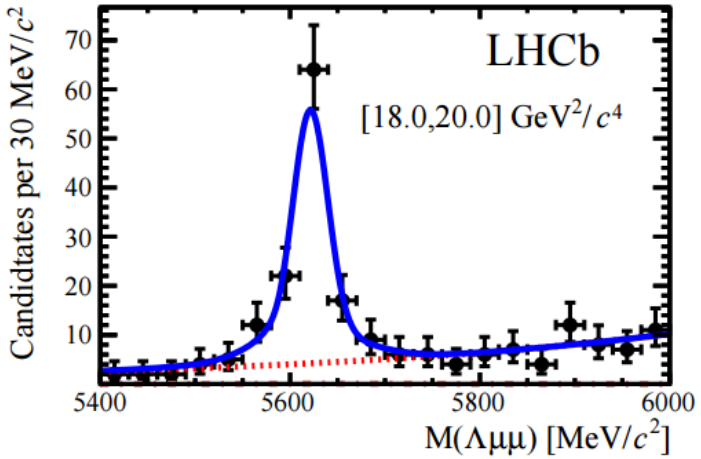

- This years LHCb measurement [JHEP 06 (2015) 115]].
- In total ~ 300 candidates in data set.
- Decay not present in the low q^2.

Angular analysis of $\Lambda_b \to \Lambda\mu\mu$

- For the bins in which we have $> 3\ \sigma$ significance the forward backward asymmetry for the hadronic and leptonic system.

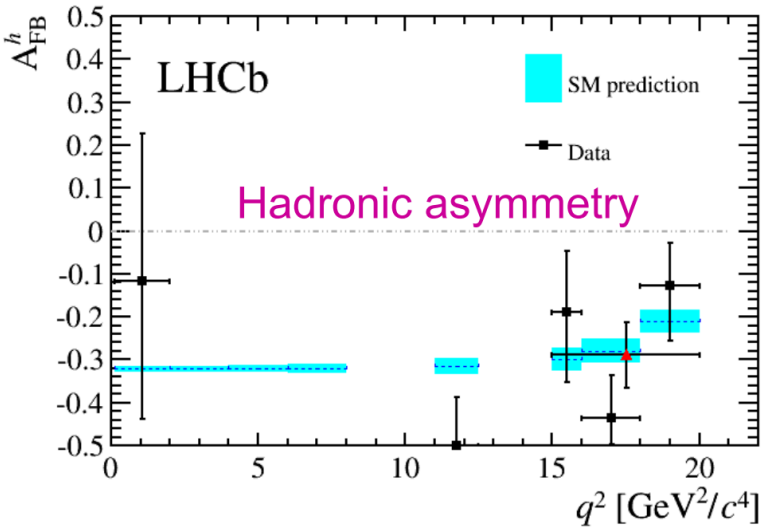

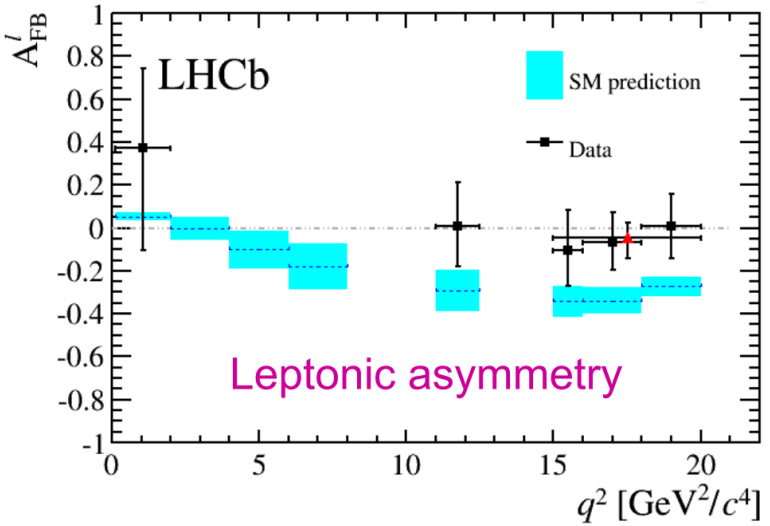

- A_{FB}^H is in good agreement with SM.
- A_{FB}^ℓ always in above SM prediction.

Lepton universality test

- If Z' is responsible for the P_5' anomaly, does it couple equally to all flavours?

$$R_{\mathrm{K}} = \frac{\int_{q^2=1\,\mathrm{GeV}^2/c^4}^{q^2=6\,\mathrm{GeV}^2/c^4} (\mathrm{d}\mathcal{B}[B^+ \to K^+\mu^+\mu^-]/\mathrm{d}q^2)\mathrm{d}q^2}{\int_{q^2=1\,\mathrm{GeV}^2/c^4}^{q^2=6\,\mathrm{GeV}^2/c^4} (\mathrm{d}\mathcal{B}[B^+ \to K^+e^+e^-]/\mathrm{d}q^2)\mathrm{d}q^2} = 1 \pm \mathcal{O}(10^{-3}) \ .$$

- Challenging analysis due to bremsstrahlung.
- Migration of events modeled by MC.
- Correct for bremsstrahlung.
- Take double ratio with $B^+ \to J/\psi K^+$ to cancel systematics.
- In $3\mathrm{fb}^{-1}$, LHCb measures $R_K = 0.745^{+0.090}_{-0.074}(stat.)^{+0.036}_{-0.036}(syst.)$
- Consistent with SM at 2.6σ.

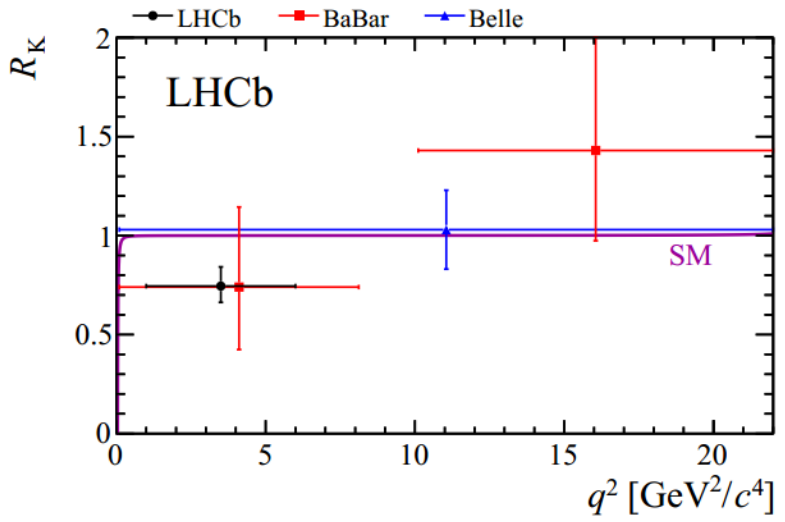

- Phys. Rev. Lett. 113, 151601 (2014)

Angular analysis of $B^0 \to K^* ee$

- With the full data set (3fb^{-1}) we performed angular analysis in $0.0004 < q^2 < 1\ \text{GeV}^2$.
- Electrons channels are extremely challenging experimentally:
  - Bremsstrahlung.
  - Trigger efficiencies.
- Determine the angular observables: F_L, $A_\text{T}^{(2)}$, A_T^Re, A_T^Im:

$$F_\text{L} = \frac{|A_0|^2}{|A_0|^2 + |A_{||}|^2 + |A_\perp|^2}$$

$$A_\text{T}^{(2)} = \frac{|A_\perp|^2 - |A_{||}|^2}{|A_\perp|^2 + |A_{||}|^2}$$

$$A_\text{T}^\text{Re} = \frac{2\mathcal{R}e(A_{||L}A_{\perp L}^* + A_{||R}A_{\perp R}^*)}{|A_{||}|^2 + |A_\perp|^2}$$

$$A_\text{T}^\text{Im} = \frac{2\mathcal{I}m(A_{||L}A_{\perp L}^* + A_{||R}A_{\perp R}^*)}{|A_{||}|^2 + |A_\perp|^2},$$

Angular analysis of $B^0 \to K^* ee$

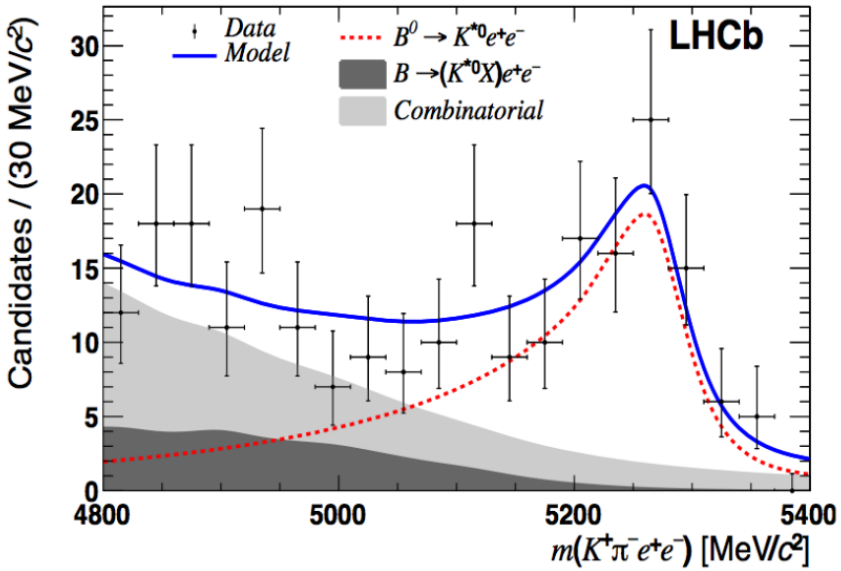

- Results in full agreement with the SM.
- Similar strength on C_7 Wilson coefficient as from $b \to s\gamma$ decays.

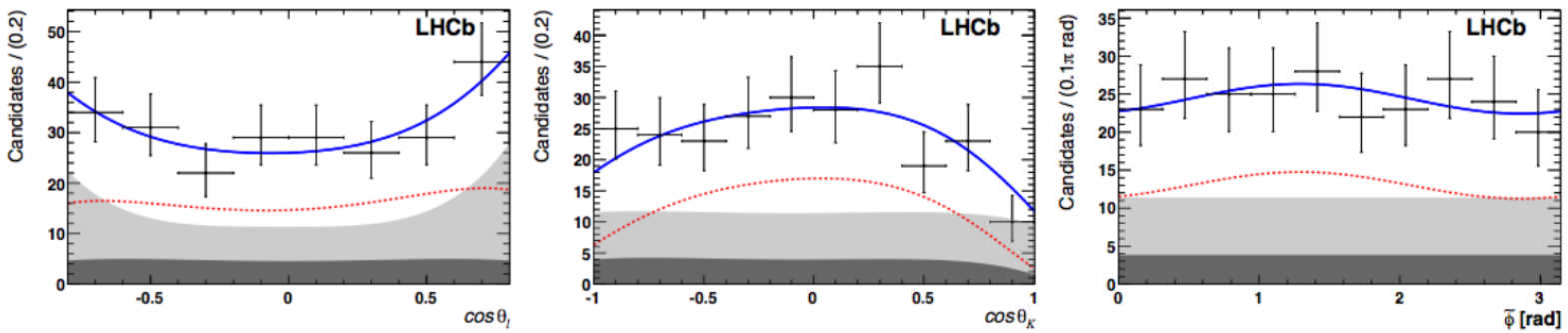

There is more!

- There is one other LUV decay recently measured by LHCb.
- $R(D^*) = \dfrac{\mathcal{B}(B \to D^* \tau \nu)}{\mathcal{B}(B \to D^* \mu \nu)}$
- Clean SM prediction: $R(D^*) = 0.252(3)$, PRD 85 094025 (2012)
- LHCb result: $R(D^*) = 0.336 \pm 0.027 \pm 0.030$, HFAG average: $R(D^*) = 0.322 \pm 0.022$
- $3.9\ \sigma$ discrepancy wrt. SM prediction

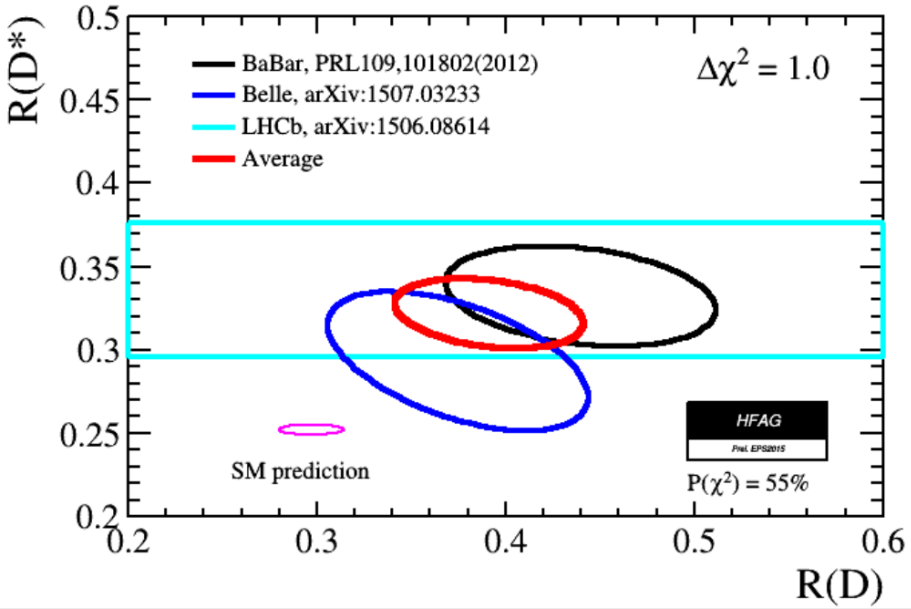

Global fit to $b \to s\ell\ell$ measurements

Link the observables

$\Rightarrow$ Fits prepare by `S. Descotes-Genon, L. Hofer, J. Matias, J. Virto`, arXiv::1510.04239

- Inclusive
  - $B \to X_s \gamma$ (BR) ..... $\mathcal{C}_7^{(\prime)}$
  - $B \to X_s \ell^+ \ell^-$ (dBR/dq^2) ..... $\mathcal{C}_7^{(\prime)}, \mathcal{C}_9^{(\prime)}, \mathcal{C}_{10}^{(\prime)}$
- Exclusive leptonic
  - $B_s \to \ell^+ \ell^-$ (BR) ..... $\mathcal{C}_{10}^{(\prime)}$
- Exclusive radiative/semileptonic
  - $B \to K^* \gamma$ $(BR,\, S,\, A_I)$ ..... $\mathcal{C}_7^{(\prime)}$
  - $B \to K \ell^+ \ell^-$ (dBR/dq^2) ..... $\mathcal{C}_7^{(\prime)}, \mathcal{C}_9^{(\prime)}, \mathcal{C}_{10}^{(\prime)}$
  - $\mathbf{B \to K^* \ell^+ \ell^-}$ $(dBR/dq^2$, **Optimized Angular Obs.**) .. $\mathcal{C}_7^{(\prime)}, \mathcal{C}_9^{(\prime)}, \mathcal{C}_{10}^{(\prime)}$
  - $B_s \to \phi \ell^+ \ell^-$ $(dBR/dq^2$, Angular Observables) ..... $\mathcal{C}_7^{(\prime)}, \mathcal{C}_9^{(\prime)}, \mathcal{C}_{10}^{(\prime)}$
  - $\Lambda_b \to \Lambda \ell^+ \ell^-$ (None so far)
  - etc.

Statistic details

⇛ Frequentist approach:

$$\chi^2(C_i) = [O_{\text{exp}} - O_{\text{th}}(C_i)]_j \, [Cov^{-1}]_{jk} \, [O_{\text{exp}} - O_{\text{th}}(C_i)]_k$$

- $\mathbf{Cov} = \mathbf{Cov}^{\text{exp}} + \mathbf{Cov}^{\text{th}}$. We have Cov^{exp} for the first time
- Calculate Cov^{th}: correlated multigaussian scan over all nuisance parameters
- Cov^{th} depends on C_i: Must check this dependence

For the Fit:

- Minimise $\chi^2 \to \chi^2_{\text{min}} = \chi^2(C_i^0)$ (Best Fit Point = C_i^0)
- Confidence level regions: $\chi^2(C_i) - \chi^2_{\text{min}} < \Delta\chi_{\sigma,n}$

⇛ The results from 1D scans:

Coefficient $\mathcal{C}_i^{NP} = \mathcal{C}_i - \mathcal{C}_i^{SM}$	Best fit	1σ	3σ	Pull_{SM}
$\mathcal{C}_{\mathbf{9}}^{\text{NP}}$	-1.09	$[-1.29, -0.87]$	$[-1.67, -0.39]$	**4.5** ⇐
$\mathcal{C}_9^{\text{NP}} = -\mathcal{C}_{10}^{\text{NP}}$	-0.68	$[-0.85, -0.50]$	$[-1.22, -0.18]$	**4.2** ⇐
$\mathcal{C}_9^{\text{NP}} = -\mathcal{C}_{9'}^{\text{NP}}$	-1.06	$[-1.25, -0.86]$	$[-1.60, -0.40]$	4.8 ⇐ (no R_K)

Theory implications

- The data can be explained by modifying the C_9 Wilson coefficient.
- Overall there is around $4.5\ \sigma$ discrepancy wrt. SM.

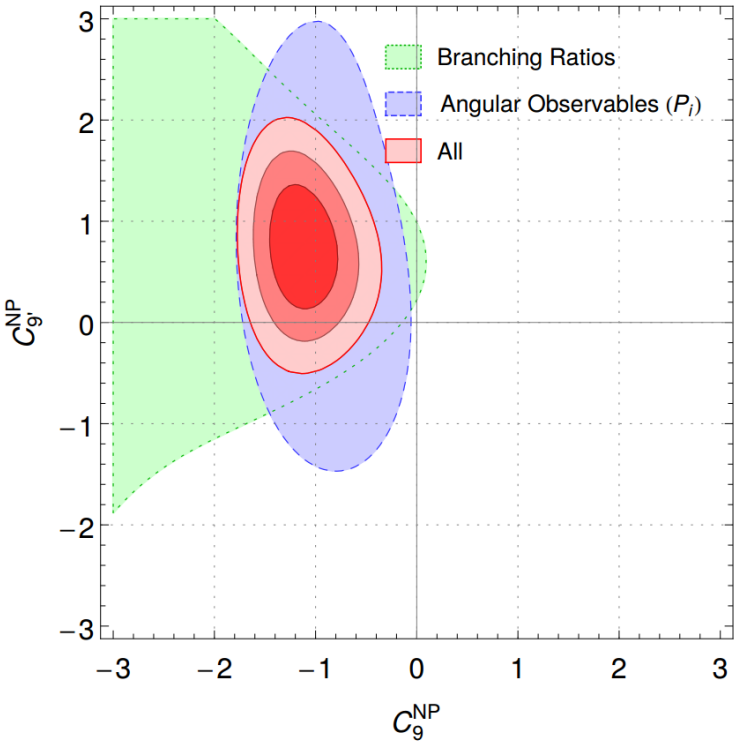

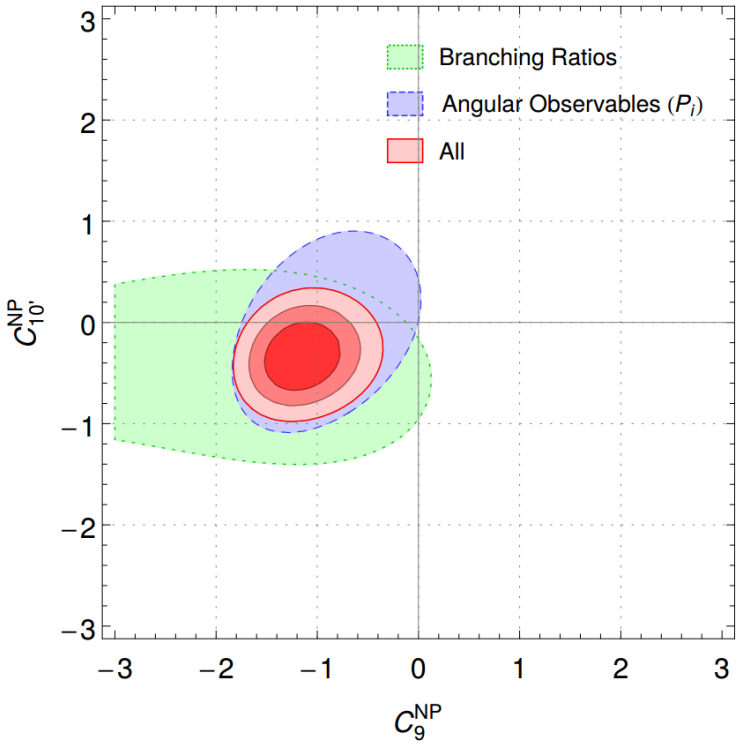

2D scans

Coefficient	Best Fit Point	Pull_{SM}
$(\mathcal{C}_7^{\text{NP}}, \mathcal{C}_9^{\text{NP}})$	$(-0.00, -1.07)$	**4.1**
$(\mathcal{C}_9^{\text{NP}}, \mathcal{C}_{10}^{\text{NP}})$	$(-1.08, 0.33)$	**4.3**
$(\mathcal{C}_9^{\text{NP}}, \mathcal{C}_{7'}^{\text{NP}})$	$(-1.09, 0.02)$	**4.2**
$(\mathcal{C}_9^{\text{NP}}, \mathcal{C}_{9'}^{\text{NP}})$	$(-1.12, 0.77)$	**4.5**
$(\mathcal{C}_9^{\text{NP}}, \mathcal{C}_{10'}^{\text{NP}})$	$(-1.17, -0.35)$	**4.5**
$(\mathcal{C}_9^{\text{NP}} = -\mathcal{C}_{9'}^{\text{NP}}, \mathcal{C}_{10}^{\text{NP}} = \mathcal{C}_{10'}^{\text{NP}})$	$(-1.15, 0.34)$	**4.7**
$(\mathcal{C}_9^{\text{NP}} = -\mathcal{C}_{9'}^{\text{NP}}, \mathcal{C}_{10}^{\text{NP}} = -\mathcal{C}_{10'}^{\text{NP}})$	$(-1.06, 0.06)$	**4.4**
$(\mathcal{C}_9^{\text{NP}} = \mathcal{C}_{9'}^{\text{NP}}, \mathcal{C}_{10}^{\text{NP}} = \mathcal{C}_{10'}^{\text{NP}})$	$(-0.64, -0.21)$	3.9
$(\mathcal{C}_9^{\text{NP}} = -\mathcal{C}_{10}^{\text{NP}}, \mathcal{C}_{9'}^{\text{NP}} = \mathcal{C}_{10'}^{\text{NP}})$	$(-0.72, 0.29)$	3.8

- C_9^{NP} always play a dominant role
- All 2D scenarios above 4σ are quite indistinguishable. We have done a systematic study to check what are the most relevant Wilson Coefficients to explain all deviations, by allowing progressively different WC to get NP contributions and comparing the pulls.

If not NP?

- We are not there yet!
- There might be something not taken into account in the theory.
- Resonances (J/ψ, $\psi(2S)$) tails can mimic NP effects.
- There might be some non factorizable QCD corrections.
  " However, the central value of this effect would have to be significantly larger than expected on the basis of existing estimates" `D.Straub, 1503.06199` .

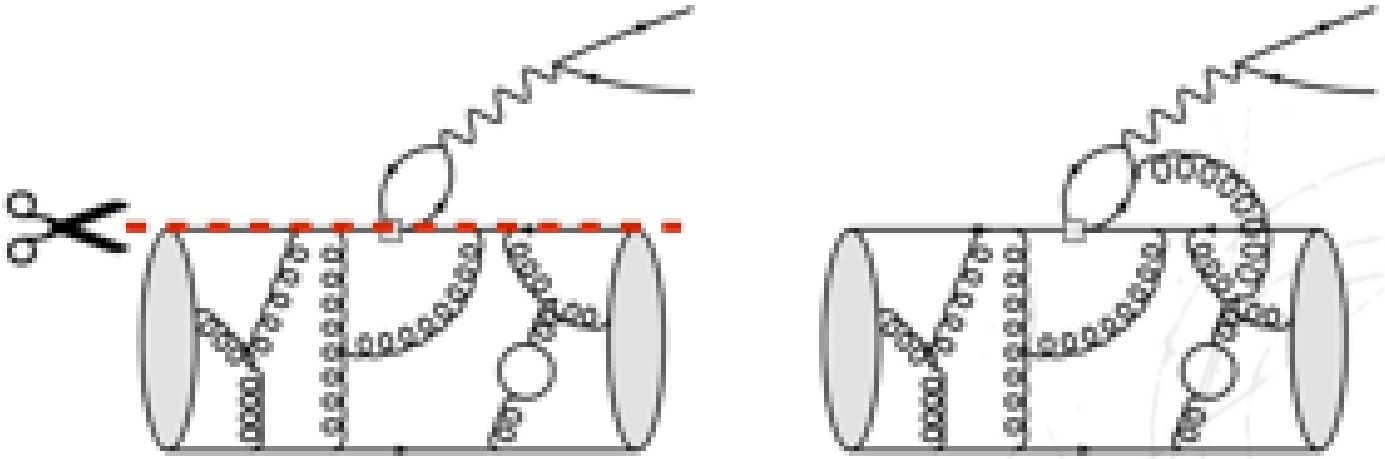

If not NP?

- We are not there yet!
- There might be something not taken into account in the theory.
- Resonances (J/ψ, $\psi(2S)$) tails can mimic NP effects.
- There might be some non factorizable QCD corrections.
  " However, the central value of this effect would have to be significantly larger than expected on the basis of existing estimates" `D.Straub, 1503.06199` .

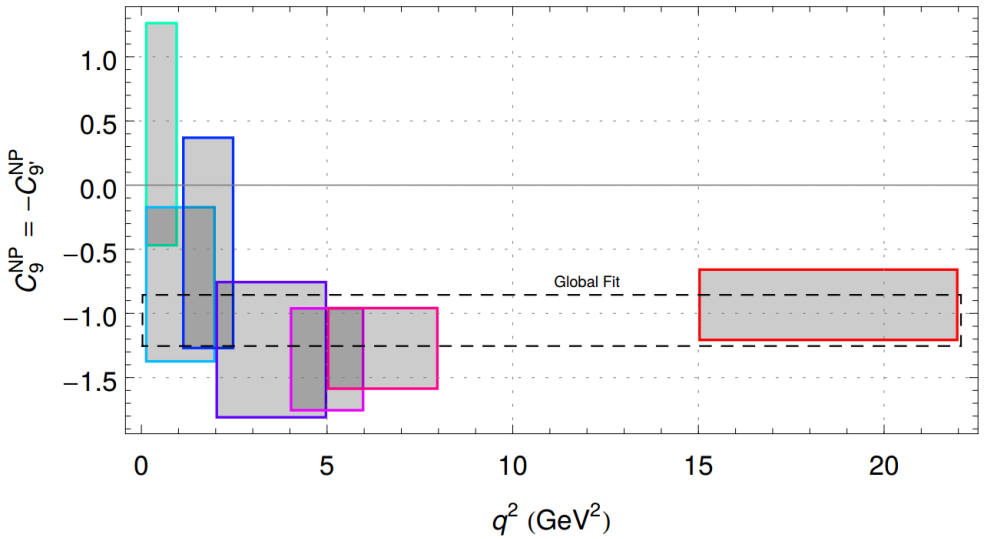

If not NP?

- We are not there yet!
- There might be something not taken into account in the theory.
- Resonances (J/ψ, $\psi(2S)$) tails can mimic NP effects.
- There might be some non factorizable QCD corrections.
  " However, the central value of this effect would have to be significantly larger than expected on the basis of existing estimates" `D.Straub, 1503.06199` .

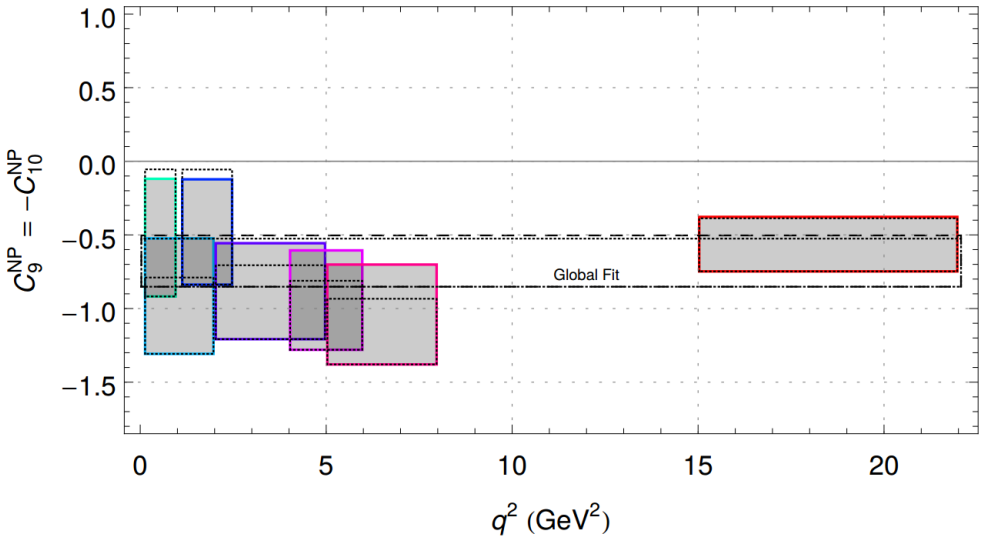

If not NP?

- How about our clean P_i observables?
- The QCD cancel as mentioned only at leading order.
- Comparison to normal observables with the optimised ones.

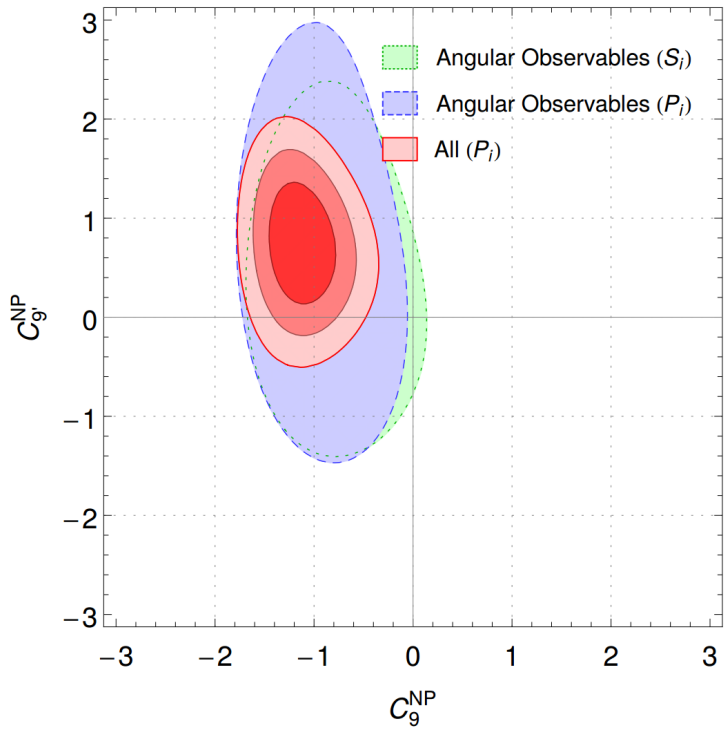

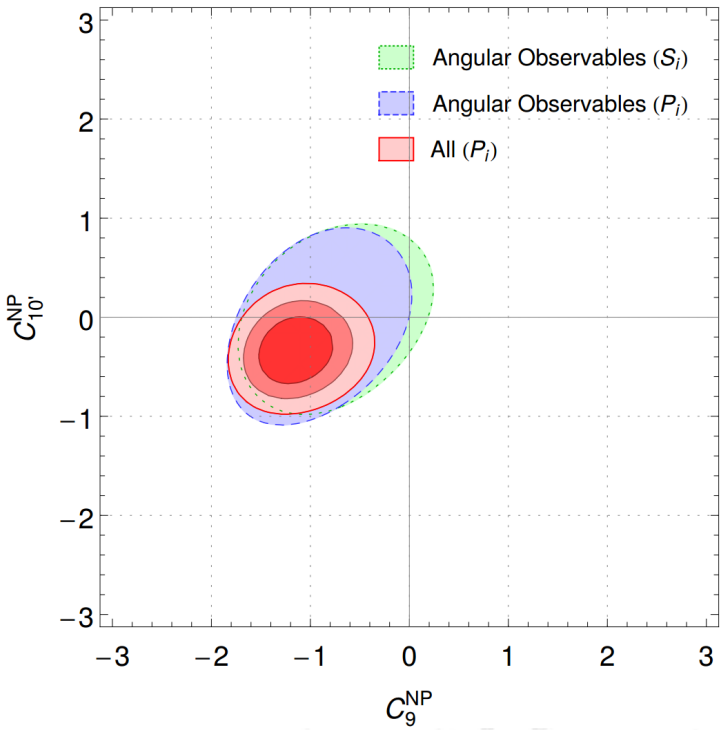

There is more!

- There is one other LUV decay recently measured by LHCb.
- $R(D^*) = \dfrac{\mathcal{B}(B \to D^* \tau \nu)}{\mathcal{B}(B \to D^* \mu \nu)}$
- Clean SM prediction: $R(D^*) = 0.252(3)$, PRD 85 094025 (2012)
- LHCb result: $R(D^*) = 0.336 \pm 0.027 \pm 0.030$, HFAG average: $R(D^*) = 0.322 \pm 0.022$
- $3.9\ \sigma$ discrepancy wrt. SM.

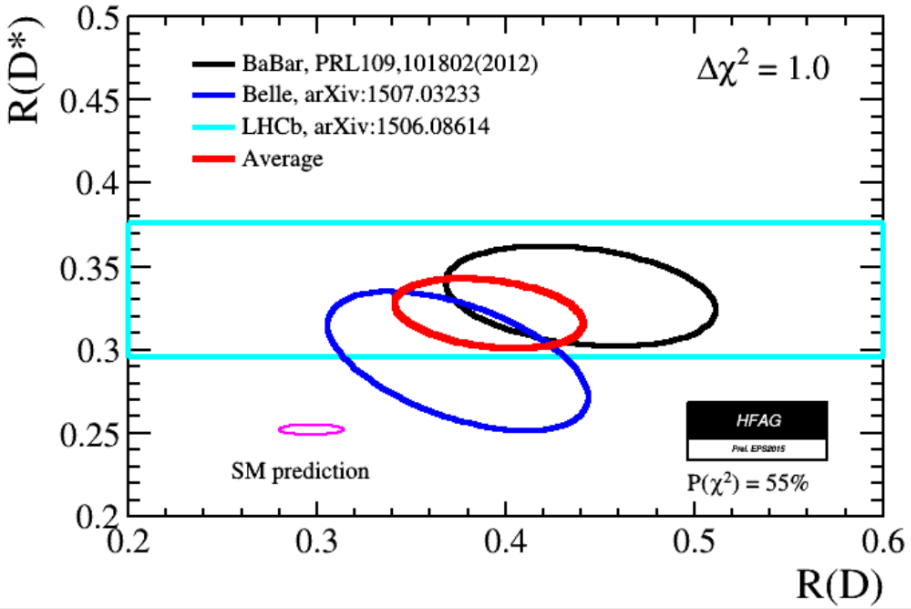

Disclaimers about some theory predictions

Disclaimer 1

$\Rightarrow$ arXiv:1512.07157, Ciuchini, Fedele, Franco, Mishima, Paul, Silvestrini, Valli

- Introduce a fully arbitrary parametrization for non-factorizable power correction:

$$\lambda \to H_\lambda + h_\lambda \text{ where } h_\lambda = h_\lambda^{(0)} + h_\lambda^{(1)} q^2 + h_\lambda^{(2)} q^4 \quad \text{and}$$
$$h_\lambda^{(0)} \to C_7^{NP}, h_\lambda^{(1)} \to C_9^{\rm NP}$$

  with $(\lambda = 0, \pm)$ (copied from JC'14).
  Complications: complete lack of theory input/output $\Rightarrow$ **no predictivity** with 18 free parameters (any shape). Specific problems...
- Because of the polynomial parametrization this is completely unphysical as it will never reproduce the amplitudes that where measured at the $B \to K^* J/\psi$.

Disclaimer 2

⇒ arXiv::1603.04355

Signal of right-handed currents using $B \to K^*\ell^+\ell^-$ observables at the kinematic endpoint.

Anirban Karan,[1] Rusa Mandal,[1] Abinash Kumar Nayak,[1] Rahul Sinha,[1] and Thomas E. Browder[2]

[1] *The Institute of Mathematical Sciences, Taramani, Chennai 600113, India*
[2] *Department of Physics and Astronomy, University of Hawaii, Honolulu, HI 96822, USA*

(Dated: March 15, 2016)

The decay mode $B \to K^*\ell^+\ell^-$ is one of the most promising modes to probe physics beyond the standard model (SM), since the angular distribution of the decay products enable measurement of several constraining observables. LHC*b* has recently measured these observables using 3 fb^{-1} of data as a binned function of q^2, the dilepton invariant mass squared. We show that LHC*b* data implies a 5σ overall signal for new physics and provides unambiguous evidence for right-handed currents, which are absent in the SM. These conclusions are derived in the maximum q^2 limit and are free from hadronic corrections. Our approach differs from other approaches that probe new physics at low q^2 as it does not require estimates of hadronic parameters but relies instead on heavy quark symmetries that are reliable at the maximum q^2 kinematic endpoint.

Disclaimer 2

⇛ arXiv::1603.04355

⇛*"The relation in Eq. (24) between form factors is expected to be satisfied in the large q^2 region. Eq. (24) is naturally satisfied if it is valid at each order in the Taylor expansion of the form factors"*

⇛ They need Eq. 24 to be valid with at least leading order at the Taylor expansion.

⇛ But this is not guaranteed as a resonant contribution can violate this expression.

The large q^2 region where the K^* has low-recoil energy has also been studied [3, 12] in a modified heavy quark effective theory framework. In the limit $q^2 \to q^2_{\rm max}$ the hadronic form factors satisfy the conditions

$$\frac{\widetilde{\mathcal{G}}_\parallel}{\mathcal{F}_\parallel} = \frac{\widetilde{\mathcal{G}}_\perp}{\mathcal{F}_\perp} = \frac{\widetilde{\mathcal{G}}_0}{\mathcal{F}_0} = -\kappa \frac{2 m_b m_B C_7}{q^2}, \qquad (24)$$

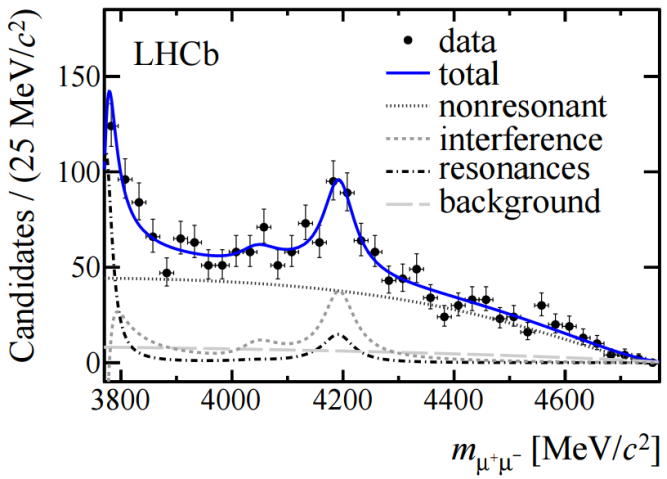

Conclusions

- Clear tensions wrt. SM predictions!
- Measurements cluster in the same direction.
- We are not opening the champagne yet!
- Still need improvement both on theory and experimental side.
- Time will tell if this is QCD+fluctuations or new Physics:

Conclusions

- Clear tensions wrt. SM predictions!
- Measurements cluster in the same direction.
- We are not opening the champagne yet!
- Still need improvement both on theory and experimental side.
- Time will tell if this is QCD+fluctuations or new Physics:

"... when you have eliminated all the
Standard Model explanations, whatever remains,
however improbable, must be New Physics."
prof. Joaquim Matias

Thank you for the attention!

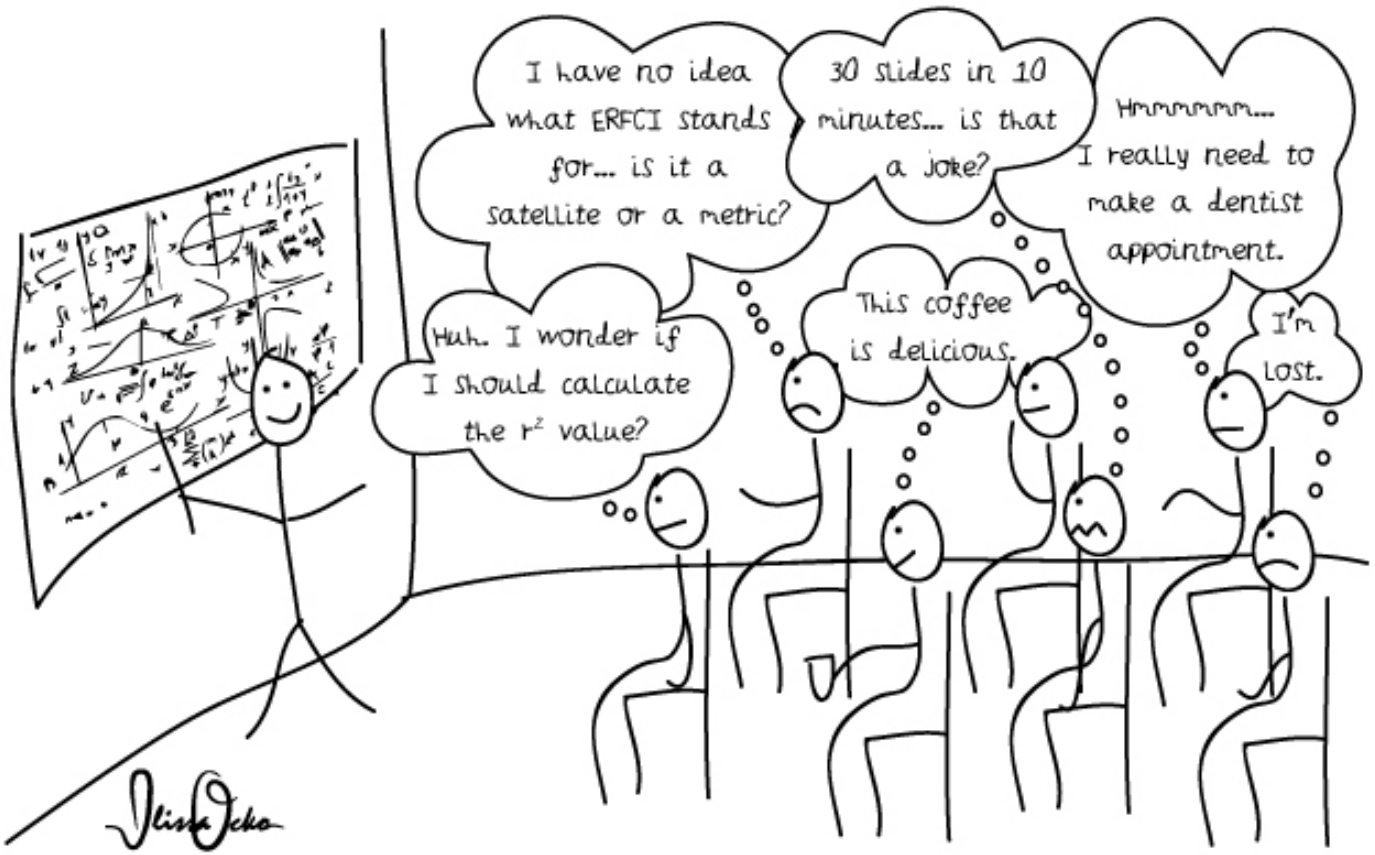

Backup